DIAGNOSIS AND PROGNOSIS OF ELECTRICAL AND MECHANICAL FAULTS USING WIRELESS SENSOR NETWORKS AND TWO-STAGE NEURAL NETWORK CLASSIFIER

by

AKARSHA RAMANI

Presented to the Faculty of the Graduate School of
The University of Texas at Arlington in Partial Fulfillment
of the Requirements
for the Degree of

MASTER OF SCIENCE IN ELECTRICAL ENGINEERING

THE UNIVERSITY OF TEXAS AT ARLINGTON
August 2008

To my family.

ACKNOWLEDGEMENTS

I would like to acknowledge and extend my heartfelt gratitude to my supervising professor, Dr. Frank Lewis, for his encouragement and motivation all through my thesis; Dr. Wei-Jen Lee and Dr. Chiman Kwan for their timely inputs and support, and Dr. Haiying Huang for agreeing to be on my defense committee. I am grateful to Prasanna Ballal, my mentor at ARRI, for helping and guiding me throughout my work. I would like to thank Matt Middleton and Chris McMurrough, without whom the thesis would not have reached its completion. I also extend my gratitude to Aditya Telang, for his assistance with my documentation. And most especially, I am thankful to my family for believing in my abilities and encouraging me to strive for greater heights; I would have never reached here but for their love and conviction.

Last but not the least, I express my gratitude to all my friends and colleagues at ARRI and UTA, who have constantly motivated me to work at the best of my potential.

This work has been sponsored by ARO grant DAAD 19-02-1-0366.

July 3, 2008

ABSTRACT

DIAGNOSIS AND PROGNOSIS OF ELECTRICAL AND MECHANICAL FAULTS USING WIRELESS SENSOR NETWORKS AND TWO-STAGE NEURAL NETWORK CLASSIFIER

AKARSHA RAMANI, M.S.

The University of Texas at Arlington, 2008

Supervising Professor: Frank L. Lewis

Diagnosis and isolation of electrical and mechanical problems in induction motors has always been a very challenging task. Some of the common problems in induction motors are: bearing, stator winding, and rotor bar failures. This thesis has three phases: The first one pertains to development of low-cost test-beds for simulating bearing faults and short circuit stator winding faults in a motor. Bearing fault is due to the failure of any of the components of the bearing and the stator winding fault is due to the failure of insulation between the windings. Bearing faults can be identified from the motor vibration signatures; where as the stator winding fault can be identified through the measurement of the fault voltage. Second, wireless modules for collection of voltage values and vibration data from the test-beds have been developed. Wireless sensors have been used because of their advantages over wired sensors in remote sensing and data collection without human intervention. Finally, a novel two-stage neural network is used to classify various bearing and short circuit faults. The first stage neural network estimates the principal components using the Generalized Hebbian Algorithm (GHA). Principal Component Analysis is used to reduce the dimensionality of the data and to extract the fault features. The second stage neural network uses a supervised learning vector quantization network (SLVQ) utilizing a self organizing map approach. This stage is used to classify various fault modes. This is followed by computation of performance metrics (Confusion Matrix, Receiver Operating Characteristics and Health Index) in order to determine the condition of the system at any instant of time and to predict the performance of the system in future. Neural networks have been used because of their flexibility in terms of online adaptive reformulation.

TABLE OF CONTENTS

LIST OF FIGURES

CHAPTER 1

INTRODUCTION

Failure avoidance is one of the main approaches for ensuring the quality and performance of a system. There are two main types of failure avoidance in terms of maintenance, namely preventive and corrective. In preventive maintenance, the focus is on keeping the equipments in good operating condition, in order for it to indicate the possible occurrence of a failure, so that actions can be taken to avert the failures [1]. In corrective maintenance, a repair is performed after a failure has occurred. Condition-based maintenance (CBM) is an approach of preventive maintenance. The process of CBM involves monitoring the system, predicting failures and making repairs before these failures occur. A system can contain many fault modes and a decision has to be taken on the type of repair necessary for eliminating any future faults.

1.1 Wireless Sensor Networks

Monitoring of the system is done using a range of sensors which can either be wired or wireless. Wireless sensors are generally used to enable remote monitoring. Wireless Sensor Networks (WSN) provide an intelligent platform to gather and analyze data without human intervention [1]. Typically, a sensor network consists of autonomous wireless sensing nodes that are organized to form a network. Each node is equipped with sensors, embedded processing unit, short-range radio communication module, and power supply, which is typically 9-volt battery. With recent innovations in MEMS sensor technology, WSN hold significant promise in many application domains.Description of the parts of a wireless sensor is as follows [2]:

- *Sensing Unit:*Consists of a sensor and an Analog to Digital Converter (ADC). The analog signals from the sensor which could be light, vibration or temperature depending on the application of the sensor is converted to digital values using the ADC.
- *Processing Unit:*Acts upon the signal sent from the sensing unit.
- *Transreceiver Unit:*Connects the sensor nodes to the network.
- *Power Unit:* For small fields, replaceable batteries are used where as rechargeable batteries are used for remote locations.

Additional units such as localization module, mobilizer unit and a power generator can be used depending upon the application. The localization module helps in finding the location of the senor node in the field [2]. The mobilizer unit connects the sensors to the mobile robots.

1.2 Condition Based Maintenance (CBM)

Condition Based Maintenance is an automatic process which determines the occurrence of a fault in the system and subsequently diagnoses the cause of it. It makes use of sensors, algorithms, models and automated reasoning for the monitoring and maintenance task. One of the biggest advantages of Condition Based Maintenance is reduction of life-cycle costs by efficient planning and effective maintenance, which in turn is brought about by understanding of the working of the equipments and the machineries. Assessing the health of machinery helps in increasing the productivity and reliability of the machine as the faults can be diagnosed and corrected on time before it takes a bigger dimension. Prior warning of an impending failure maximizes effectiveness of the maintenance repair and minimizes downtime and resource requirement. CBM technology also provides significant savings compared to preventive maintenance based systems on run-to-fail-maintenance [3]. In order for a condition based maintenance system to be effective, it should operate as a system which detects and classifies the incipient faults, predicts the remaining life cycle of the equipment, supports the operator's decision for the course of action; interfaces with the control system to take action; aids the maintainer in making repairs; and provides feedback to the logistics support and machinery design communities [3].

1.3 Wireless Sensor Network for Condition Based Maintenance

Real time data interpretation which is one of the primary ingredients of CBM are systems which mature with time. Distributed date acquisition which is another important aspect of CBM, should hence be appropriate for both maintenance and monitoring systems. Details on this can be obtained from [1]. Wireless Sensors help in providing a component in controlling the machinery as well as for identifying the system. Wireless Sensors have an edge over the conventional wired systems in terms of being installed in hazardous, restricted and difficult to reach areas.

The WSN help in collecting data from the various distributed sensors such as accelerometer, temperature sensors, light sensors etc. which could then be used for diagnostic and prognostic purposes. The results obtained through the running of these data are compared with the stored fault pattern library in order to diagnose faults and eventually upgrade the existing fault pattern library. The final step involves estimating the Remaining Useful Life of the equipment which would be useful to the maintenance personnel.

1.4 Related Work

Diagnosis and isolation of electrical and mechanical problems in induction motors has always been a very challenging task. Some of the common problems in induction motors are: bearing problems, followed by stator winding failures and rotor bar failures, out of which bearing faults account for 40% of all the failures. Since the bearings carry the weight of the rotor, its fault diagnosis becomes very important [4]. Vibration monitoring is one of the methods used for bearing fault analysis. Vibration monitoring for the critical power plant components has been used for a number of years. There are several things that need to be kept in mind for online health monitoring systems [5]. Signals that can help in diagnosis and prognosis must be identified through the right type of sensors and supporting instrumentation. Basic signal processing techniques which can highlight the fault signature and suppress the dominant system dynamics and noise must be taken into consideration. The final step should be the development of detection and decision making process for prognosis. There are many challenges that need to be faced before successful implementation of diagnosis and prognosis, for example, for an induction motor the magnetic flux distribution is the best indicator for the stator winding fault, but this requires a good magnetic sensor to be fixed inside the motor, which could prove to be expensive and a difficult task. Therefore, a solution for this could lie in measuring the fault current, which should be analyzed properly for detection and decision making, but there are certain problems such as: a) The fault signature, i.e., the stator current is $50 - 80dB$ smaller than the signals themselves [5].In such cases, even the manufacturing defects could be treated as fault signals. b) The other problem faced is due to the fact that no two machines have identical characteristics, even if they are from the same assembly line. Therefore, systems need to be developed which can overcome these problems. There are two ways in ways in which the bearing maintenance can be done:

1. By estimating the bearing life based on statistical methods. But this is not a very appropriate method as there could be post manufacturing defects that might give a wrong estimated life span based on the statistical analysis of experimental data. Their inaccuracy also lies in the fact that they do not work real time to give the results. Therefore, we go for the second method.
2. Bearing condition monitoring and diagnosis, where signal processing techniques can be used for real time monitoring. This is generally done using two types of information - vibration and acoustics and secondly, current and electromagnetic flux information.

Some of the fault diagnosis techniques which have been proposed have been discussed in the following section.

1.4.1 Model Based Technique

In Model Based technique, a mathematical model is tried to fit into a mechanical system. They match the vibration response of the system due to the faults present in the bearing [6]. These models are system dependent and require true knowledge of the system being modeled [6]. In the technique proposed in [7], the description of the vibration produced by a single point defect on the inner race of a rolling element bearing under constant radial load was done with the help of a model. The bearing geometry, shaft speed, bearing load distribution were some of the features incorporated by the model suggested. The model helped in comparing the predicted and demodulated vibration spectra.

1.4.2 Time-Domain Technique

Time Domain analysis is one of the simplest methods for detecting incipient bearing faults. It can be done either visually or by applying some statistical parameters such as Crest factor, Root Mean Square Value, Kurtosis Value etc. These have a greater value when the machine is under fault compared to the faultless condition. Parameters like crest factor and kurtosis give spikiness of the signal and not the vibration magnitude. Initially, the crest factor and kurtosis increase as the spikiness of the vibration increases, but as the damage increases the vibration becomes random and these values move towards normal values. Thus, the time domain analysis lacks the ability to track the defects in the later stages of the fault. Time domain analysis technique to detect the bearing faults was used in [8] and [9]. The skew values of rectified data and the kurtosis values of the unrectified data were used to detect the bearing fault. These results were independent of load and speed variations. In [9] statistical parameters (Crest Factor and Skew) were used to detect vibration and sound pressure signals to detect the bearing defects. Even beta distribution function was used in the same paper but it was inferred they did not prove to be very helpful in identifying different types of bearing defects.

1.4.3 Frequency Domain Technique

In Frequency Domain Analysis frequency components and their amplitudes are used for detecting bearing faults. The FFT of signal is analyzed, which shows peaks and harmonics in the vibration spectra at the bearing defect frequency in the event of a fault. These peaks show a marked increase as the severity of the fault increases. When there are a large number of frequency components in the spectrum and the signal to noise ratio is low, it becomes difficult to distinguish between the faults and the noise components. This therefore, becomes a drawback. *Envelope Analysis*, also known as *High Frequency Resonance Technique* has been used to overcome this problem which has been studied in [10]. It is based on the concept that every time the raceway is hit by a localized defect, an impulsive force gets generated exciting the resonance of the mechanical system between the point of impact and the point of measurement. This method helps in getting the amplitude modulation of the resonance which lets the location and detection of the defect to be known.

1.4.4 Time-Frequency Domain Analysis

Time-Frequency Domain Analysis uses both time and frequency domain information to detect the transient features such as impact. There are a number of time-frequency domain techniques such as Short Time Frequency Transform (STFT), the Wigner-Ville Distribution (WVD) and the Wavelet Transform (WT). In cases where the signal to noise ratio is low and there is a presence of a lot of frequency components, these time-frequency domain techniques prove to be useful in detection of faults as explained in [11].

In [5], a solution for bearing outer race failure and faults due to stator voltage imbalances have been suggested, where the concept of machine modeling along with wavelet and symbolic dynamic analysis has been used for early detection of faults in an induction motor. Development of sensor fusion technique gives a probabilistic approach to these problems in induction motors. The method extends the D-Markov process to combine the information from both electrical and mechanical sensors. The vibration data that is obtained is analyzed using Continuous Wavelet Transform which has been discussed in detail in Chapter 6. Parks vector modulus has been computed on the signals that have been obtained from the machine under consideration, which converts the instantaneous 3-phase stator current (R^3) signals into orthogonal reference frame (R^2) and then again this value is converted to a single value (R) using a modulus operator. The time domain signals that are obtained from the above method is analyzed using wavelet transform. This is then followed by Markov machine construction, which lets compression of information and helps is giving an accurate measure of the fault. This measurement of fault leads to an estimate of the health of the machine.

There may be certain disadvantages of using CWT in analysis: 1) there is a problem of redundancy associated with CWT- the calculation of the wavelet transform is done by continuously shifting a continuously scalable function over a signal and calculating the correlation between the two. These scaled functions do not give an orthogonal basis function and hence, result in redundancy. This may sometimes not be looked as a great disadvantage because making a signal orthogonal, reduces the Signal to Noise Ratio. 2)There are an infinite number of wavelets present in the wavelet transform which have to be reduced to a smaller amount for further analysis. 3) For most of the wavelet transform, analysis can be done only mathematically and hence it poses a limitation. This makes it necessary to use Discrete Wavelet Transform. But the use of DWT for analysis makes the signal no longer shift-invariant, which means that the time shifted version and the wavelet transform of the same signal are not shifted versions of each other.

In [12], Multi-Resolution Analysis using wavelet technique has been used to identify thermal degradation or degradation via electrical charge of the bearing, where an increase in the characteristic frequencies can be captured when the bearing undergoes degradation. The MRA calculates the general RMS trend for the measured vibration signals from the bearings. The higher frequencies dominate the signal when the motor becomes old and hence, gives an indication of bearing damage. The MRA therefore, gives the bearing information without distorting the original signal. Hence, this paper proposed a method to find the age of the three phase squirrel cage motor through analysis of the vibration spectra from the bearings.

In [13], wavelet transform based bearing-localized defect detection has been presented, where, wavelets are applied to detect the periodic structural ringing due to repetitive impulsive forces created when rolling element passes over a defect. This proposed a method which reduced the compromise on frequency resolution for time localization.

1.4.5 Higher Order Spectral Analysis

Higher Order Spectral Analysis which describes the degree of correlation among different frequencies present in the signal can also be used for fault detection. When there are large values of phase correlation among the harmonics of defect frequency, it indicates some bearing fault. Bicoherence has been used for analysis in the research work [14] which helps in extraction of the features determining the condition of the bearing. Bicoherence has been used to find the degree of phase correlation among any three harmonics of the bearing characteristic defect frequencies.

1.4.6 Fuzzy Logic

Diagnosis of the frequency spectra of the bearing fault can also be done with the help of fuzzy logic if the input is processed in the right way as mentioned in the work presented in [15]

1.4.7 Neural Network (NN) Based Techniques

Neural Network Approach makes use of pattern identification technique to detect the bearing faults. Vibration monitoring using neural networks has been done in [16] [17]. The extracted features from the vibration signals are used for training the network, which in turn is used to match the condition of the bearing. Analysis using Artificial Neural Network (ANN) is very useful when a large amount of data needs to be classified. Data classification (*pass* or *fail*) using ANN helps in letting the user know whether the data can be used for further analysis. Since it does not require development of decision rules, its more adaptable to decision rules[18]. Some of the advantages of using ANN are:

1. The weights used in ANN make it more robust compared to the Decision trees.
2. The performance of ANN is improved through learning, which continues even after the application of training set.
3. The error rate is low and the accuracy is high after the training.
4. They are more robust in noisy environments.

Some of the applications of ANN are:

- Statistical Modeling
- Image Compression
- Optical Character Recognition
- Medical diagnosis based on some symptoms
- Industrial Adaptive Control

In the analysis proposed in [19], a multi-layered feed forward NN trained with Error Back propagation technique and an unsupervised Adaptive Resonance Theory-2 (ART2) based NN was used for detection and diagnosis of localized faults in ball bearings. The NN was trained using the statistical parameters obtained from the signals under faultless and fault condition. The state of the ball bearing was obtained from the output of the Neural Network.

In this thesis, we have made use of a two stage Neural Network through which online adaptive reformulation is possible. This method eliminates the need for the entire set of data to be present for classification as opposed to back propagation method and hence, saves on the processing time if the volume of data is large. Principal Component Analysis for feature extraction used in the first stage of NN is advantageous compared to statistical methods as it avoids batch processing. The proposed algorithm works well both with linear and non-linear systems in comparison to Radial Basis Function and back propagation methods, which work best when the system is linear. The analysis used in this work is more accurate compared to time domain and frequency domain techniques.

1.5 Problem Definition

The work in this thesis puts forward a method for machine maintenance and monitoring through signal processing techniques by measuring the vibration and fault current. A wireless sensor network with advanced prognostic capability for monitoring critical power plant components has been proposed. The proposed system combines the hardware and the prognostic software in a unified framework which will subsequently reduce the system downtime and the maintenance cost. The data collection part consists of the test-beds (for generation of fault signals) and wireless sensors and modules (for recording the fault information), and a Personal Computer (for storing the fault values for analysis). The analysis involves using Artificial Neural Network based approach which would help in identifying the degraded state of the system or more precisely, it helps in determining the point at which the degradation has begun. ANN has been used because of its good functional approximation property and extraordinary ability on pattern recognition.

The advantages of the proposed system are:

- **Saving in installation cost** The proposed WSN system can be set up in a short time of around 1 hour and has a low installation cost. This is much lesser compared to cost of wired network which ranges from $10-1000$ per foot. The buffer and the sampling rate of these sensors can be kept high.
- **Continuous and Real Time Collection of Data** Since the sensing is continuous and real time, the failures can be detected at an early stage itself. Hence, it is helpful in preventive maintenance.
- **Low Cost** The sensors which have been used in the experiment are inexpensive. Hence, their usage saves on the cost.
- **Portable hardware processor with state-of-the-art prognostic algorithm** The data can be measured on a continuous basis with the help of the sensors. Even a Data Acquisition Card can be used to record the data on a continuous basis on a PC.
- **Use of Advanced Prognostic Tools** Prognostic tools like ANN, and Hidden Markov Model can be used for prognosis for Condition Based Maintenance.
- **Performance of the Algorithm used** The performances of these prognostic algorithms used have been proved through various researches that have taken place in the similar field.

The work also proposes a novel two-stage neural network to classify various short circuit and bearing faults. The first stage neural network estimates the principal components using the Generalized Hebbian Algorithm (GHA). Principal Component Analysis is used to reduce the dimensionality of the data and to extract the fault features. This gives the flexibility of updating the principal components online as new data comes in. The second stage neural network uses a supervised learning vector quantization network (SLVQ) utilizing a self organizing map approach. This stage is used to classify various fault modes. Neural networks have been used because of their flexibility in terms of online adaptive reformulation. In the end, a discussion on the performance of the proposed classification method has been done.

The preceding section 1.4 gave an insight into the various researches that have gone in the field with a brief introduction to the work that is going to be explained in the forthcoming chapters. The second chapter explains in detail the experimental set up for the the mechanical and electrical test beds, the wireless modules and sensors used in these test beds for measuring the signals. The third chapter provides information regarding the various time domain techniques and their application to the signals that have been recorded for the experiment. The fourth chapter describes the various frequency domain techniques and the manner in which they have been used for the data obtained from the two test beds. Fifth chapter gives in detail the Principal Component Analysis and the two stage neural network used in this thesis. Sixth chapter describes the various classification techniques. The results are presented in the seventh chapter followed by conclusion and future work in the eighth chapter.

CHAPTER 2

EXPERIMENTAL SET UP OF THE TEST BEDS

One of the prime focus of this thesis is development of test beds for recording signals from the machines for “Condition Based Maintenance”. Therefore, this along with the appropriate selection of sensors for the experimentation forms an important part. This chapter is broadly divided into three sections and hence, explains: a) Induction Motor- its working principle, parts and types of internal faults in it. b) The detailed description of experimental set-up of the two test beds - electrical and mechanical, and c) The wireless modules and sensors used in the experiment.

2.1 Induction Motor

The Induction Motor is a type of AC motor where, power is supplied to the rotor by means of electromagnetic induction. Because of the relative motion between the rotor circuits and the rotating magnetic field produced by the stator windings, a torque is produced which causes the rotation. The following sections give an insight into the operation and the fault types in Induction Motors.

2.1.1 Working Principle of AC Induction Working

The AC induction motor is a rotating electric machine which operates from a three phase alternating voltage source. The induction motors are so called because the current in the rotor conductors are supplied by induction. The three phase stator has three windings which are displaced by 120°. When currents flow through the three symmetrically placed windings, a sinusoidally distributed air gap flux generating the rotor current is produced. The rotor conductors are cut by the alternating field in the stator set up by the alternating supply, thereby inducing alternating current in the armature conductors. The interaction of this sinusoidally distributed air gap flux and induced rotor currents produces a torque on the rotor to give the mechanical output. The electromechanical interaction between the stator and the rotor also constitutes transformer action. More details can be found in [5]

2.1.2 Construction

Figure 2.1 [12] shows the parts of an Induction motor.

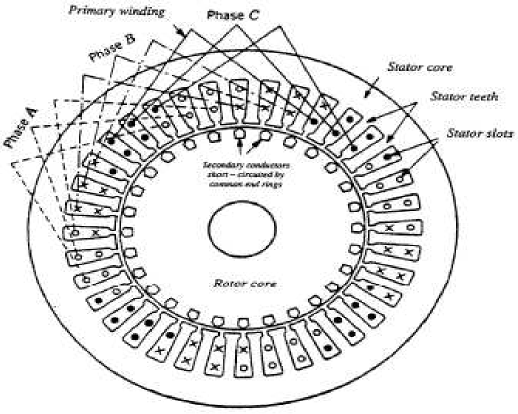

Figure 2.1 Parts of an Induction Motor

The two main parts of the induction motor are:

- *Stator*
- *Rotor*

The stator consists of a core of stacked, insulated, iron laminations with Polyphase windings of insulated copper wire filling the slots in the core. The windings of the stator are such that they produce an air gap magnetic motive force which is symmetrically distributed around the magnetic poles. The rotor also consists of a core of stacked, insulated, iron laminates. The slots are filled by aluminum bars or copper windings. There are two types of rotors:

- *Squirrel Cage Rotor*
- *Slip-Ring Rotor*

Squirrel Cage Induction Motor

The name comes because of its shape: a cylindrical cage comprised of axial bars terminated in annular rings. Cast Aluminum is used for the bars and the end rings. The conductors are generally skewed along the rotor length to reduce the noise and torque fluctuations. The thin laminations reduce the eddy current losses.

Slip-Ring Induction Motor

In this case the rotor windings are made up of wire and have the same number of poles as the stator winding. Electrical connections are made from the rotor to the ring. Brushes which are in contact with the rings transfer electric power to the exterior part such as variable resistor which can help changing motor's slip rate. These require more maintenance and are more expensive compared to squirrel cage induction motor.

2.1.3 Internal Faults in an Induction Motor

The faults in induction motor can be categorized as electrical or mechanical faults. Electrical faults can be further sub-divided into stator or rotor faults. The mechanical faults are the faults associated with the bearings of the machine [5].

2.1.3.1 Stator Faults

The stator faults pertain to the short circuit or open circuit of the stator windings. Short circuit of the windings are caused due to

- failure of the winding insulation between turns within a phase coil
- failure of the winding insulation between turns of different phases
- failure of insulation between a turn and the stator core

The failure of insulation may be because of thermal, mechanical, chemical or environmental stress.

- Thermal stresses are caused due to: overloading, unbalanced phase voltages, obstructed ventilation and high ambient temperature.
- Electrical stresses are due to excessive voltages which are caused due to: switching induced over voltages, lightening and variable frequency drives. This would eventually lead to the breakdown of the dielectric.
- Mechanical stresses develop due to the relative motion between the coil bundles and the stator, leading to loss of insulation. It can also be developed due to relative motion of the conductors arising from vibration or magnetic forces.
- Environmental stresses are caused due to moisture, chemicals and foreign particles present in the atmosphere.

2.1.3.2 Rotor Cage Faults

The rotor is subjected to much lower voltages and much higher temperature compared to the stator windings. Therefore, the most common failure mode in rotors is open or broken rotor bar. This in turn can be caused due to mechanical, thermal or residual stresses. Much of the thermal stresses in rotor are due to it design and construction. The mechanical causes are magnetic forces, vibrations and shock which is much greater than what the stator is subjected to. The rotor gets affected by only those stresses which affect its geometry. These stresses can be present in any of the planes-tangential, radial or axial. Whenever there is a transition from no load to loaded condition, the stresses produced result in a change in the rotor geometry and hence, produce vibrations.

2.1.3.3 Bearing Faults

Bearing faults are the most common faults occurring in all the machines probably because of the reason that they carry the weight of the rotor. Rolling bearings generally consist of two concentric rings (called the outer raceway and inner raceway, respectively) with a set of rolling elements running in their tracks. The rolling elements come in the following standard shapes: the ball, cylindrical roller, tapered roller, needle roller, and symmetrical and unsymmetrical barrel roller [5]. In order to have uniform spacing and for prevention of mutual contact, the rolling elements in a bearing are guided in a cage. The rolling element type is the most common bearing type which can be seen in the figure 2.2 [5]. Each component of the bearing can undergo a failure in order to cause the fault. Some of the causes of this fault are:

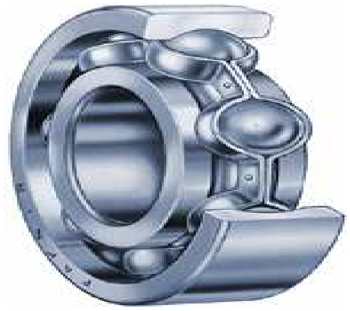

Figure 2.2 Cross Section of a Rolling Element Ball Bearing

- **Mechanical Damage**: Improper handling of the bearings results in dents and nicks, causing displacement of the metal particles which can introduce secondary effects in the motor when they indent the raceway. Even brinelling (permanent indentation due to overload) might occur due to improper mounting techniques.
- **Damage due to wear**: The wear and tear in the bearings may result in gradual deterioration producing conditions which may become prominent for the bearing failure in the long run
- **Corrosion Damage**: This kind of damage comes into picture when the motor is operated in a moist atmosphere. The moisture in the air causes surface oxidation and rusting, paving the way for abrasion and crack initiation.
- **Crack Damage**: This occurs when the motor is subjected to large stresses through overloading or cyclic loading. Cracks may also be produced because of manufacturing defects and improper heat treatment and grinding.

- **Electric Arc Damage**: Bearings can be damaged when the grounding of the equipment is not done properly. An arc is produced between non contacting elements and its runways when current passes through it resulting in damage.
- **Damage due to lubricants**: It is caused due to improper lubrication system of the bearings which is present as the lubrication between the rolling elements and the raceways.

2.2 Test Beds

2.2.1 Electrical Test Bed

This test bed aims at monitoring the short circuit current faults in a motor by analyzing the input current of the motor. The stator coils of the motor have been simulated by connecting inductors of different sizes (1 mH, 2.5 mH, 5 mH, 10 mH, 20 mH, 30 mH) in series. The conceptual design of the entire electrical test bed setup can be seen in figure 2.3 The test bed has the following capabilities:

- **Fault Location:** It can simulate the fault at the beginning of the coil, middle of the coil, and end of the coil.
- **Fault Duration:** Varying the length difference of the make-break contact can adjust the duration of the fault. This was brought about by varying the length of the two metallic strips used for getting the short circuit spark.
- **Faults Severity:** We can short 1 mH inductor for low level fault or 30 mH inductor for severe fault. In addition, we can also adjust the value of the variable resistor to simulate the bolded fault or resistance faults. In case of resistance fault, the severity is more as the presence of resistance increases the spark produced and hence the current and the corresponding voltage.

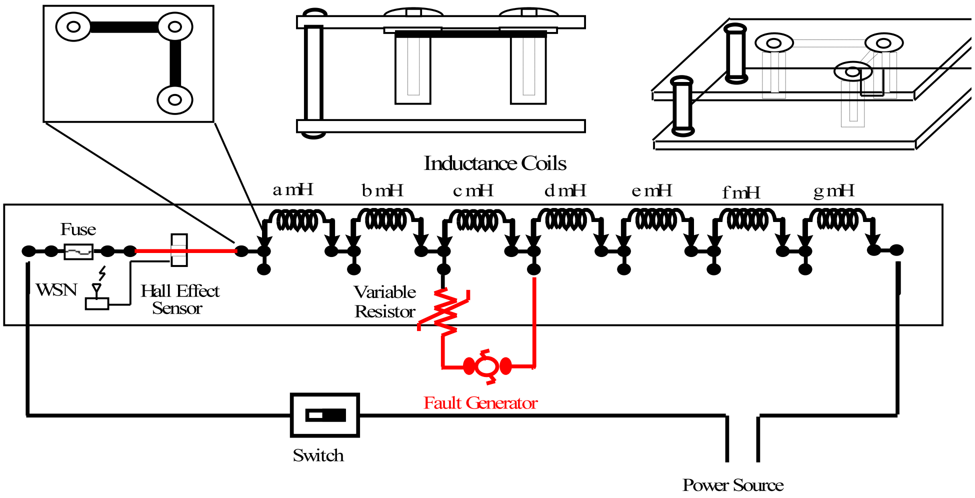

Figure 2.3 Conceptual Design of the test-bed for electrical faults

- **Data Collection:** The data will be recorded through wireless modules.

The experimental set up as shown in the block diagram figure 2.4 aims at collecting the profile for different cases of fault current by recording the input current of the motor at each case and by observing the severity of the fault at different values of the inductances measured at the beginning, middle and end of the series inductance coils. The total inductance of the coil in the test bed is $68.5mH$ which has been split into the following inductance values: $30, 20, 10, 5, 2.5$ and $1mH$. When the data is recorded with the inductance in the beginning of this $68.5mH$ coil, it is called the beginning of the coil, when placed in the middle (in the case of the middle of the coil, the inductances on either side should be approximately same, i.e., for $20mH$ in the middle, the distribution of inductances should be:

$30, 20, 10, 5, 2.5$ and $1mH$) it is called the middle of the coil and when placed at the end of $68.5mH$, it is called the end of the coil. The fault generator as shown in figure 2.5 has the following characteristics:

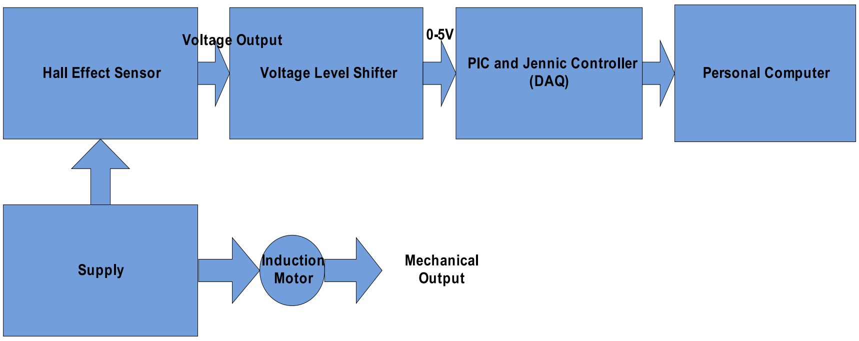

Figure 2.4 Experimental Set-Up for the Electrical Test-Bed

1. This is capable of simulating an arcing fault of a 4 pole machine with a speed of 1800 rpm (with 60 metal poles; each with a rating of 30 rpm).
2. The duration of the fault can be adjusted by varying the length difference of the make break contact. It can be either in the beginning, middle or at the end of the inductance coil.
3. A variable resistance can be inserted to simulate the bolded fault.

Since the input current to the motor is high, the data obtained cannot be directly recorded by the Wireless Modules. Therefore, we make use of Hall Effect Sensor which converts the current to a small voltage value. The Hall Effect Sensor

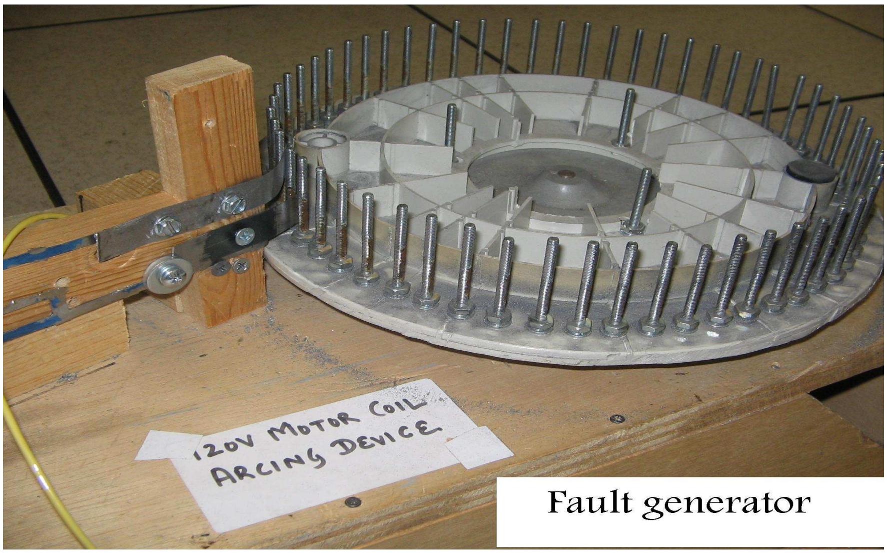

Figure 2.5 Induction Coils Simulating the Fault Generator

used is L03S050D15-L03S series. Figure 2.6 shows the Hall Effect Sensor that has been used for the experiment.

The secondary output range of this sensor is -4 to +4 Volts which can be easily detected by the Wireless Modules. It is based on the principle of production of magnetic flux proportional to the current flowing in the coil. The sensor measures this magnetic flux which is produced without any contact with the primary circuit; as a result of which no voltage drop is produced in the measured circuit which provides excellent galvanic isolation. Some of the features of this Hall Effect Sensor are:

- Zero Insertion Loss
- Measures both AC and DC
- Galvanic Isolation between the primary and the measuring circuit

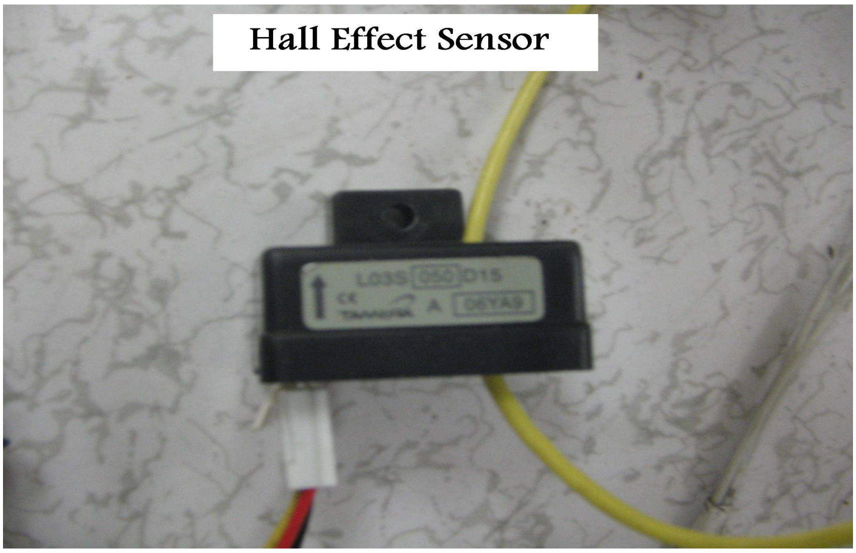

Figure 2.6 Hall Effect Sensor

- Quick Response.

Some of the specifications of this sensor are:

- Operating Temperature : -10° - 80° C
- Response Time : 5μ sec
- Output Linearity : ±1 %
- Frequency Bandwidth: -3dB

The Wireless Modules can read only the positive values, hence an operational amplifier is used for DC voltage level shifting. The OP-AMP used for the experiment is OPA227-DIP8. Figure 2.7 shows the pin diagram of the Op-Amp used. OPA227 is an industry standard series operational amplifier which combines low noise (3nV/$\sqrt{Hz}$) and wide bandwidth (8MHz, 2.3Vμ s) with high

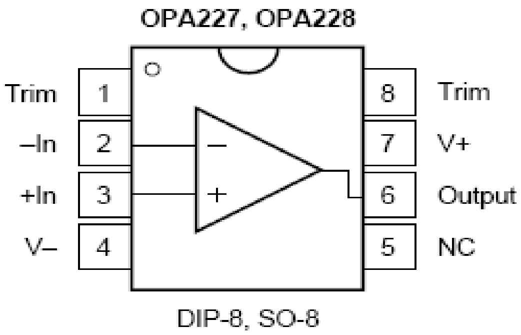

Figure 2.7 OPA-227 Pin Layout

precision to be used for AC and DC precision performance. The OPA227 is unity gain stable and features high slew rate. Some other features of this OP-AMP are:

- Small settling time: 5μ sec
- High CMRR: 138dB
- High Open Loop Gain: 160dB
- Low Input Bias Current: 10nA max
- Low Offset Voltage: 75μV max
- Wide Supply Range: ±2.5V to ±18V
- Available as single dual and quad versions

OPA227 is ideal for professional audio equipment. It is also good for portable applications requiring high precision because of its low cost and low quiescent current. The other applications where it can be put into use are:

- Data Acquisition
- Telecom Equipment
- Geophysical Analysis
- Vibration Analysis
- Spectral Analysis

- Active Filter
- Power Supply Control

The operational amplifier is connected to an analog interface circuit which does the level shifting for the analog input obtained through the Hall Effect Sensor. This level shifting is required because the wireless modules can record only positive values. The analog interface circuit consists of the operational amplifier along with resistors and capacitors which act as the *RC* filter. Figure 2.8 shows the analog interface circuit used for the voltage level shifting of the input obtained from the Hall Effect sensor. An offset voltage of $2V$ is given to the operational amplifier.

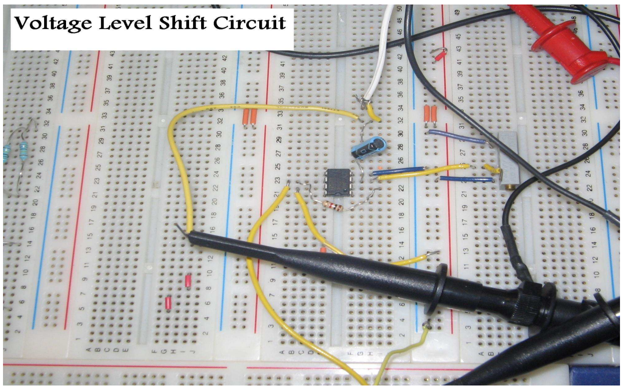

Figure 2.8 Voltage Shifting Circuit using Op-Amp 227

2.2.2 Mechanical Test Bed

For a particular bearing geometry, the rolling elements in the bearing produce vibration spectra which have unique frequency components. These frequency components along with their magnitude help in determining the condition of the bearing. The test bed for the mechanical fault consists of a motor to which a flywheel is attached figure 2.9. The most important element of this test bed is the flywheel which has holes drilled on it (as shown in figure 2.11), because it actually simulates the corrupted bearings of the motor. The weights applied to these holes produce the imbalance in the flywheel. The holes are drilled in three concentric rings-inner, middle and outer.

The severity of the fault is determined by the location of the weight-the highest being when the weight is applied on the outermost ring and vice versa. The disc, therefore acts as the load to the motor, with the screws (weights) simulating the mechanical fault at the bearings of the motor. The increase in the addition of the weight increases the rotational frictional loss of the rotor which in turn would increase the total loss in the motor and hence reduce the efficiency of the machine. There is an imbalance in the system when center of mass of the rotor/shaft system is not centered along the axis of rotation [12]. Another reason for the imbalance in the motor is also a shift in the center of gravity of the flywheel when weights are added to it. The motor rotates in order to reduce the effect of this shift so that

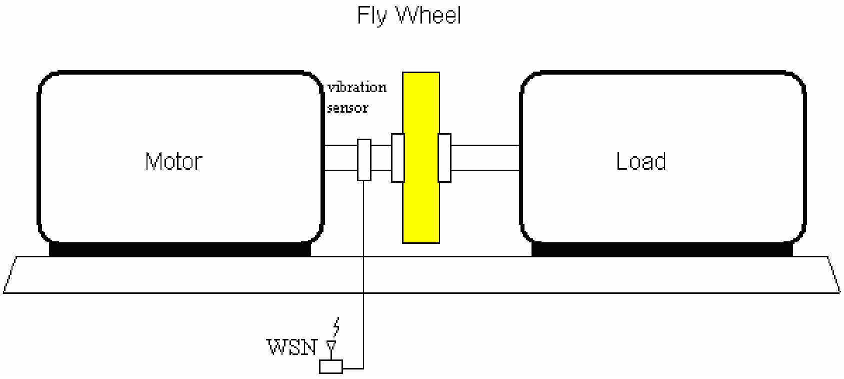

Figure 2.9 Conceptual design for the mechanical test-bed

the entire weight acts through the center of the body. The mechanical test bed consists of measuring the vibration produced from the machine in which a fault has been created. The vibration that is produced when loads are added to the disc is because of the pitting of the ball in the bearing which causes a deflection in the radial direction. This pitting can also cause the ball to lose its pure rolling condition to give tangential acceleration. The term "acceleration" actually means the deviation of the operating speed (positive or negative) from the normal operating speed. The other cause of the vibration is the manner in which the motor is coupled to the outside system. The entire setup is enclosed in a metallic cage for the purpose of safety when the loads are attached to it as shown in the figure 2.10.

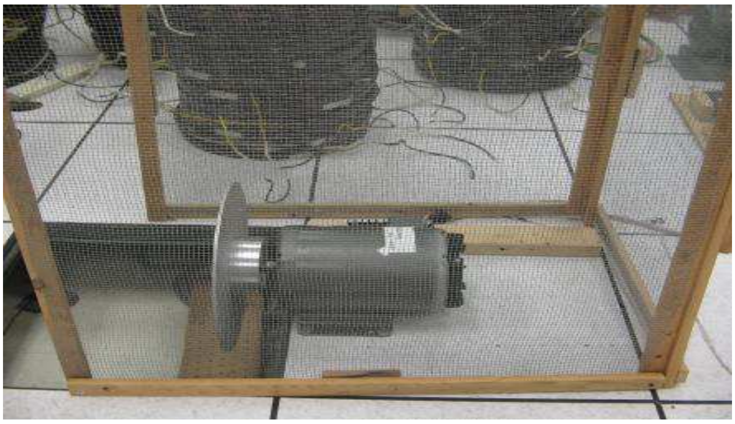

Figure 2.10 Enclosed Setup for the experiment

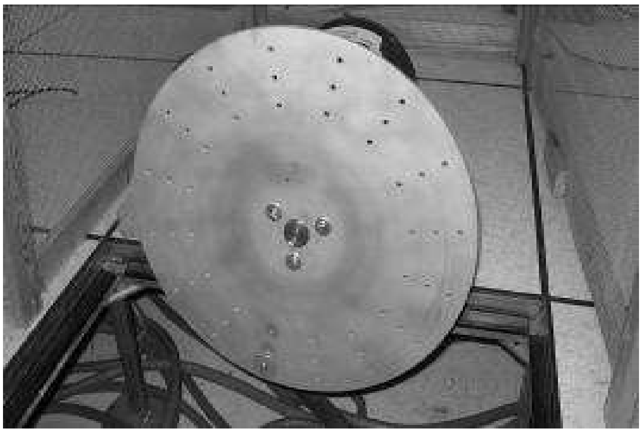

Figure 2.11 Metallic Disc with drilled holes

2.3 Wireless Modules and Sensors

The recording of the data for the electrical test bed is done by the wireless modules-$PIC18f4550$ and the Jennic. The data from the wireless modules is stored on the PC with the help of RealTerm terminal software. The values obtained are in ASCII which are converted to analog values (with the help of MATLAB code) for analysis. The sampling rate of the Wireless Module is $1.2KHz$. A custom PCB, designed at ARRI, has been used for the wireless sensing. After the fabrication of the board by a third-party company, they were manually populated with surface mount components in the lab. The remote sensing board contains a Microchip $PIC18F4550$ microprocessor running at $20MHz$ connected to a Jennic wireless micro controller module. Some of the features of $PIC18F4550$ controller are:

- **Alternate Run Modes:** Power consumption during code execution can be reduced by as much as 90% by clocking the controller from the Timer1 source or the internal oscillator block.
- **Multiple Idle Modes:** The controller can also run with its CPU core disabled but the peripherals still active. In these states, power consumption can be reduced even further, to as little as 4 of normal operation requirements.
- **On-the-fly Mode Switching:** The user can incorporate power-saving ideas into their applications software design through power-managed modes which are invoked by user code during operation.
- **Low Consumption in Key Modules:** The power requirements for both Timer1 and the Watchdog Timer are minimized.
- **Memory Endurance:** The Enhanced Flash cells for both program memory and data EEPROM are rated to last for many thousands of erase/write cycles up to $100,000$ for program memory and $1,000,000$ for EEPROM. Data retention without refresh is conservatively estimated to be greater than 40 years.
- **Self-Programmability**: These devices can write to their own program memory spaces under internal software control. By using a bootloader routine, located in the protected Boot Block at the top of program memory, it becomes possible to create an application that can update itself in the field.
- **Extended Instruction Set**: The $PIC18F4550$ family introduces an optional extension to the PIC18 instruction set, which adds 8 new instructions and an Indexed Literal Offset Addressing mode. This extension, enabled as a device configuration option, has been specifically designed to optimize re-entrant application code originally developed in high-level languages such as C.

- **Enhanced CCP Module**: In PWM mode, this module provides 1, 2 or 4 modulated outputs for controlling half-bridge and full-bridge drivers. Other features include auto-shutdown for disabling PWM outputs on interrupt or other select conditions and auto-restart to reactivate outputs once the condition has cleared.
- **Enhanced Addressable USART**: This serial communication module is capable of standard RS-232 operation and provides support for the LIN bus protocol. Other enhancements include Automatic Baud Rate Detection and a 16-bit Baud Rate Generator for improved resolution. When the micro controller is using the internal oscillator block, the EUSART provides stable operation for applications that talk to the outside world without using an external crystal (or its accompanying power requirement).
- **10-bit A/D Converter**: This module incorporates programmable acquisition time, allowing for a channel to be selected and a conversion to be initiated, without waiting for a sampling period and thus, reducing code overhead.
- **Dedicated ICD/ICSP Port**: These devices introduce the use of debugger and programming pins that are not multiplexed with other micro controller features. Offered as an option in select packages, this feature allows users to develop I/O intensive applications while retaining the ability to program and debug in the circuit.

This module transmits in the $2.4GHz$ spectrum using the 802.15.4 wireless protocol. In this setup, the PIC micro controller is dedicated entirely to collecting the samples using its on board analog to digital peripheral and then transmitting them through its UART peripheral to the Jennic module for wireless transmission to the computer. The Jennic is responsible for receiving the incoming serial data and transmitting it as quickly as possible. Previously attempts were made to use only the Jennic which has its own analog to digital peripheral, but the module by itself was too slow to handle the data collection and transmission functions together.

The receiving end consists of another Jennic module that receives the samples and outputs a digital representation on the UART. The UART of the Jennic module is connected to the computer's serial port via a TTL-RS232 converter. Jennic uses the ZigBee protocol which is a low cost protocol widely used in wireless sensing.

The firmware for this project consists of the programs running on both the PIC and the Jennic modules. The Jennic firmware was created using the freely provided Jennic SDK. The firmware is based on a Jennic provided application note that provides interrupt-driven transmission of serial data over the wireless radio. On the receiving end, the firmware on the Jennic formats the sample data in a manner to make it easier to parse and use by the computer application. The PIC firmware was developed using the CCS compiler for mid-range PIC micro controllers. This firmware was optimized to collect 8-bit samples at a rate commensurate with the bandwidth of the RF link. As the samples are collected at the desired sample rate, they are stored in a FIFO buffer and sent to the Jennic module as the UART becomes available.

This wireless board also has many other capabilities not utilized in this project. Originally, it was designed and used for autonomous aerial vehicle control. In addition to collecting analog data, it is also capable of interfacing to sensors that use simple general purpose IO or synchronous serial buses including I2C. It is also capable of driving its IO pins to logic levels and generating PWM signals for possible control applications. Figures 2.12 and 2.13 show the Wireless Modules.

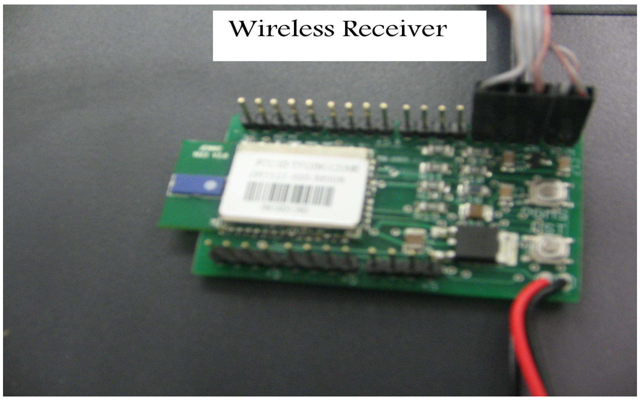

Figure 2.12 Jennic Wireless Module

The implementation of the electrical test bed consists of measuring the voltage values from the motor under fault for different values of inductances $(30, 20, 10, 5, 2.5, 1mH)$ over a period of five days. The "faultless" condition pertains to the case where there are no inductances added to the coil of the motor, where as the "faulty" condition pertains to the readings taken when the external inductances are added to the coil of the motor. The voltage is given by the equation:

$$V = IX_L \tag{2.1}$$

where, V gives the output voltage, I is the short circuit current for the machine under fault and X_L is inductive reactance which is given by:

$$X_L = j \times \omega \times L \tag{2.2}$$

and, $\omega = 2 \times \pi \times f$. From the equation 2.1, it can be inferred that as the value of the inductance increases, the output voltage value increases, which can be easily

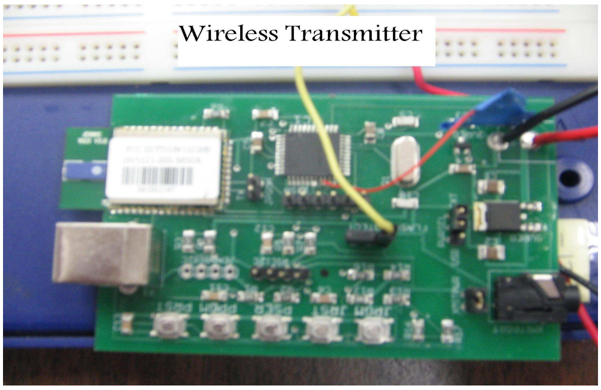

Figure 2.13 PIC 18F4550 Module

seen in the values recorded during the experiment- the voltage values for a $30mH$ inductance is greater than the voltage values obtained for $10mH$ inductance. The supply frequency is constant at $60Hz$.

In the case of bolted fault a resistance (rheostat of 10 Ohms) is included in the circuit to increase the fault level further. Now, the V becomes $V = I(X_L + R)$.

2.3.1 Vibration Measurement

For a particular bearing geometry, the rolling elements in the bearing produce vibration spectra which have unique frequency components. These frequency components along with their magnitude help in determining the condition of the bearing. In the mechanical test bed, recording of the data consists of measuring the AC and the DC component. The DC component which is used to check for the input DC current of the motor is recorded by the Ultrasonic Sensor, Ultra-Trak 750 (figure 2.14), whose output is connected to the PIC wireless modules. Since, the wireless modules cannot be directly attached to the rotating flywheel, Ultra-

Trak sensor is used which helps in issuing warning of a mechanical failure of the system by detecting changes in ultra sonic amplitude. Because of its low current and demodulated output, the Ultra-Trak sensor can be connected to alarms or data loggers. It can be mounted in any type of environment because of its stainless steel covering and water and dust resistance properties. Wide dynamic range and sensitivity adjustment facilitates its use in many sensing environments. Some of the special features of this sensor are:

- Demodulated output for analysis
- Dynamic Range: 120dB
- Sensing Range: 40dB
- Peak Frequency Response: 40 kHz
- Outputs for External Data Logging or Sound Recording
- IP 64 Rated

2.3.1.1 Working of Ultra-Trak 750

The Ultra-Trak senses the high frequency emissions produced by the motor. Once a baseline threshold is set (within a wide range of 120dB), the Ultra-Trak monitors the changes in the ultrasonic amplitude within a range of 40 decibels. This sensor can be connected to other devices which can issue an alarm or it can be used to track potential problems. It can be used for sound level increases as in the case of detecting bearing failures.

This Ultra-Trak sensor is then connected to the $PIC18f4550$ and the Jennic wireless micro controller whose details have already been explained in the previous section.

G link Micro strain sensors have been used to measure the three dimensional (radial, axial and tangential) components of the vibration. The G link sensors con-

Figure 2.14 Ultra Trak 750 Sensor

sists of triaxial MEMS accelerometer and Analog devices $ADXL202$ or $ADXL210$. These accelerometer nodes have data logging transceivers in order to be used in high speed wireless networks. Figure 2.15 shows the sensing node which detects the vibration values and the figure 2.16 shows the receiver unit which sends the output to the PC to which it is connected. Since every node in the wireless network has a unique 16 bits address, therefore, a single host transceiver can cater to many sensing nodes. These sensors with bi-directional RF communication link can be used up to a range of $70m$ for line-of-sight and $300m$ with the optional high gain antenna. The host PC can also log in data on a real time basis from up to 16 nodes simultaneously in $2.4GHz$ range. This sensor has a flash memory of $2MB$ and with a sweep rate of $2kHz$. The transceiver communicates with the PC using a serial port having a baud rate of $115.2kBd$. It uses an open communication architecture $IEEE802.15.4$. The acceleration range of this sensor is $\pm 2g$ or $\pm 10g$. Some of its other features are:

- Resolution: 200 μg/Hz
- Data Logging Points: Up to 1000000 data points at $32Hz$ to $2048Hz$.

- Measurement Accuracy: $10mg$

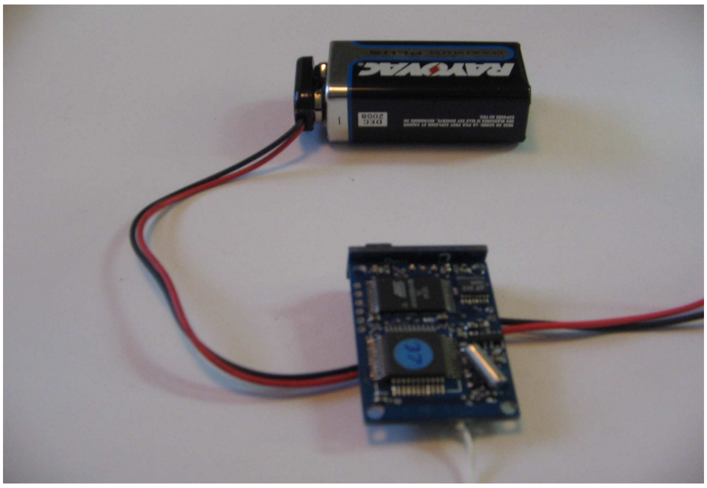

Figure 2.15 Accelerometer Sensing Node for recording 3D values

Some of the applications of G-Link Wireless Accelerometer Node are:

- Condition Based Maintenance by Wireless Sensor Networks
- Sports performance and sports medicine analysis
- Assembly line testing with smart packaging
- Security Systems enabled by wireless sensor networks
- Inclination and Vibration Testing and control

Figure 2.17 shows the arrangement of the sensor for recording the three dimensional vibration data from the motor. This arrangement is chosen to maintain uniformity in x, y and z values obtained each time of the experiment.

The implementation involves recording the three dimensional vibration data from the motor over a period of five days. The vibration data is measured for conditions of no weight as well as for weights of $5g$, $10g$, $15g$, $20g$ applied on the inner,

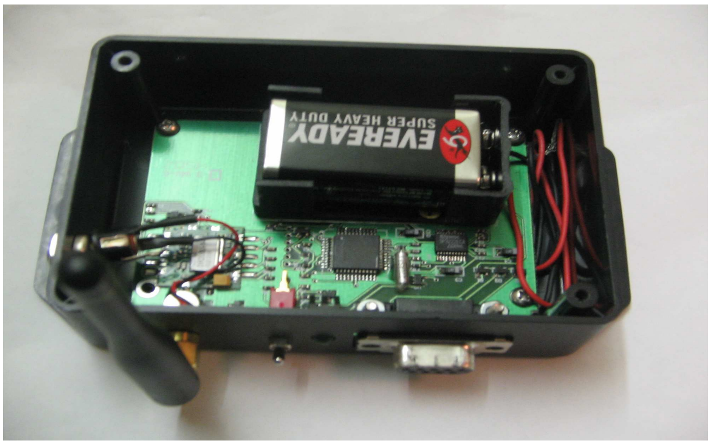

Figure 2.16 Transceiver Unit of the Glink accelerometer

middle and outer rings of the flywheel respectively. Each experiment (for a particular weight and its position on the flywheel) is performed five times.“Faultless” condition pertains to the reading taken when there are no weights added to the disc, where as “faulty” condition pertains to the reading recorded when the various weights are added to the disc. The data recorded is then used for PCA estimation and prediction of the motor condition for fault prognosis. While performing the experiment itself it was clearly seen that the vibrations produced were more when higher weights like 20 g were placed than when lower weights like $5g$ was placed on the inner ring.

Initially, Crossbow sensors with Lab View interface were used for the real time data acquisition, but because of their sampling rate limitation; the PIC wireless modules were used for the experimentation. Some of the disadvantages of using the Wireless Motes were:

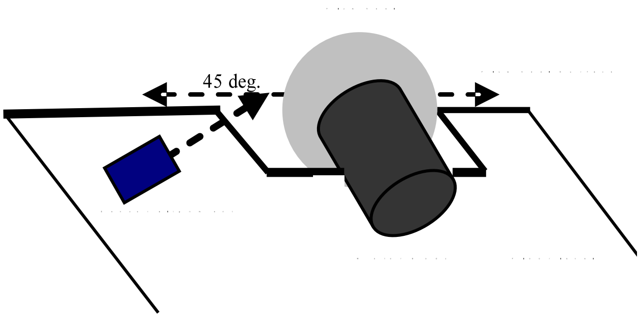

Figure 2.17 Diagram showing alignment of sensor with respect to the motor

1. Large amount of data cannot be stored in the buffer of the Mica motes, which posed a sampling rate limitation on their usage. The data recorded is stored in the queue which when retrieved do not reproduce the input signal and resulting in data loss. The wireless modules used in the experiment, (have a maximum sampling rate of 100k-which cannot be used because of data transmission limitations) can be used for a higher sampling rate and hence, help in overcoming this problem of data loss.
2. The wireless modules used in the experiment can be used up to a maximum voltage of $5V$ where as, the Mica2 motes can be used for a maximum voltage value of $3V$.

Both the Mica2 motes and the wireless modules used for the experiment can work only on DC.

CHAPTER 3

INTRODUCTION TO TIME DOMAIN ANALYSIS

Analysis of any signal with respect to time is called “Time-Domain” Analysis. Analysis of the voltage and vibration signals, as in the case of this thesis in the time domain is one simplest method of detecting faults. This can be done either visually or by examining some statistical parameters like RMS, crest factor and Kurtosis value. These parameters act as trend parameters for detecting incipient bearing faults. Their values are higher for fault conditions rather than faultless condition. This chapter describes the various time domain techniques such as Probability Density Function, Correlation, Convolution, etc. and also shows the outputs that were obtained when these methods were performed on the signals obtained from the motor under consideration.

3.1 Time Domain Analysis

Analysis of signals obtained from the “faulty” machines requires extraction of feature parameters, in which the knowledge of the system dictates the number of feature space dimensions. The better the system is, the easier monitoring and diagnostics become. The selected features must be robust and noise free for further analysis. Time domain analysis is one of the methods of feature extraction. Time Domain as the name suggests pertains to the analysis of a mathematical function with respect to time. The signals recorded at any point of time from the machine can determine the condition of the machine, for e.g., high impulses can be seen for a higher fault intensity etc. For this thesis, time domain parameters have been extracted as a part of pre-processing stage to examine the fact whether these signals recorded can be used for further analysis. Figures 3.1, 3.2 and 3.3 show the output of a machine under "faultless" and "fault" conditions respectively.

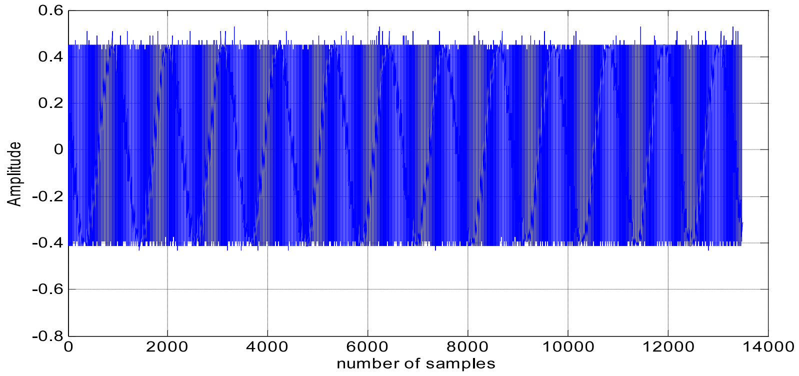

Figure 3.1 Voltage values in the faultless condition

From the figures it can be clearly inferred that the number of spikes (harmonics) are more in the faulty case as compared to the "faultless" case. This (presence of spikes) can be used as an indication for the fault condition. Greater the number of spikes, more is the severity of fault. Figure 3.3 shows the voltage value for the "bolted" fault, where a resistance is added to increase the fault level. Statistical parameters can be used for extraction of time domain features, which in turn provide information about the probability density distribution of the data. This probability density function gives the amount of spikiness in the data, which in turn gives the extent to which the fault is present in the system. Peak and Root Mean Square are also measures with which the time domain parameters can be extracted. Details on this can be found from [4]

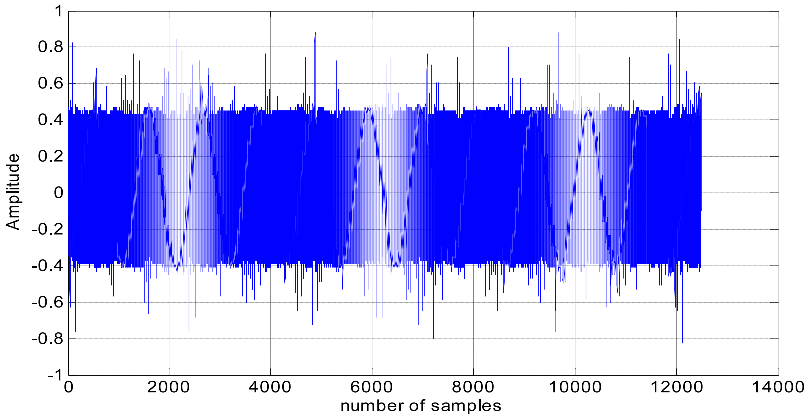

Figure 3.2 Voltage values in solid fault condition

3.1.1 Probability Density Function

Probability density function gives the distribution of probability in terms of integrals. A series of vibrations which can be superimposed onto a random background vibration and can be modulated with the bearing rotation are produced due to the discontinuity of the material on the surface of the bearing raceways. And in the case of electrical fault, as the value of inductance increases from $1mH$ to $30mH$, the voltage level increases (the increase in the value of the inductance increases the inductive reactance which in turn increases the fault voltage level). These impulses quickly decay in time due to the damping effect on the bearing material. The severity and the location of the faults can be assessed with the pattern of the fault that is generated. For example, the signals obtained at the starting of a defect is going to be different from the signals obtained under severe fault condition in either case.

The amplitude characteristics of the signals $(X(t)$, which is assumed to be sta-

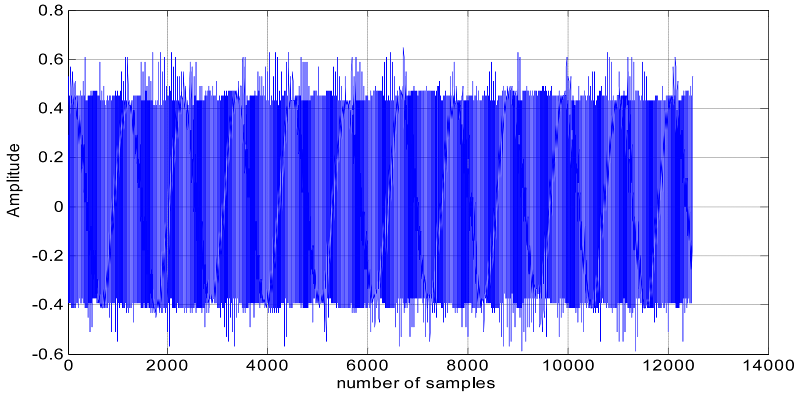

Figure 3.3 Voltage values in resistance fault condition

tionary for random processes) obtained from the faulty machine can be expressed in terms of probability density function (PDF). More information can be found in [4]. This PDF is found out by determining the time period for which a signal remains in a set of amplitude window.

$$P(x \leq X(t) \leq x + \delta x) = \sum_{i=1}^{N} \frac{\delta t_i}{T} \tag{3.1}$$

where

δt_i is the time duration of the signal ($X(t)$) obtained from the machine falling into the amplitude window (δx). T is the total time duration of the signal. Equation 3.1 can be used for health monitoring of the machine. The normalized PDF of the signals from the machine does not vary with load and speed but changes as the condition of the bearing deteriorates as in the case of mechanical fault or changes as the value of fault inductance increases, as in the case of electrical fault. The tails of the PDF broaden as the damage increases. Large spread at low probabilities and high values of PDF at the median give a highly impulsive time domain waveform. The probability returns to the basic Gaussian form, once the spall has spread over most of the working surface of the bearing element as in the case of mechanical fault. Figures 3.4 and 3.5 show the probability density function for a faultless and a faulty case respectively. *Kernel Smoothing function* has been used in each of the cases to compute the probability density function. The graph obtained under faultless condition is closer to the Gaussian curve and has a tail that is less broad compared to the plot obtained under fault.

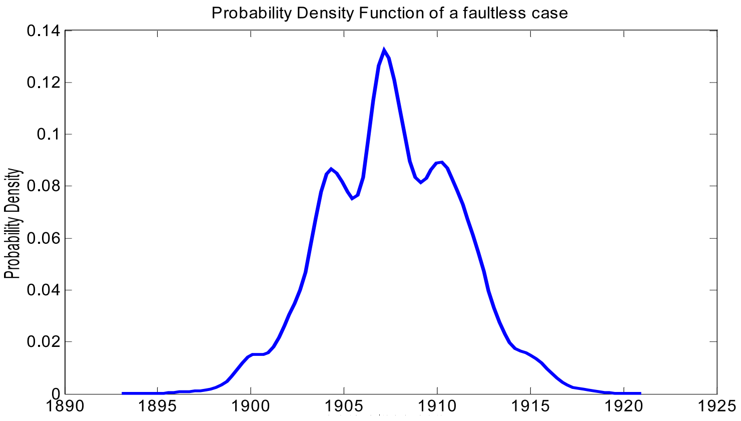

Figure 3.4 Probability Density Function of a faultless case

3.1.2 Root Mean Square and Peak Value

Root Mean Square (RMS) also known as *quadratic mean* is the statistical measure of the magnitude of a varying quantity. It is very useful in case of sinusoidal waves. It is used to indicate the energy levels of the vibration signals. The

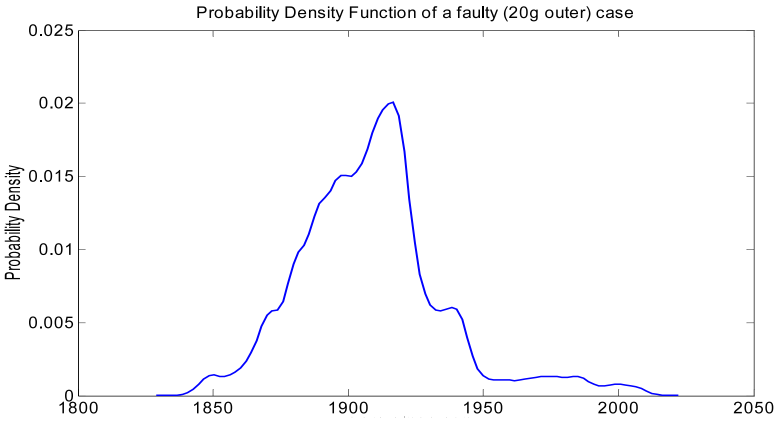

Figure 3.5 Probability Density Function of a faulty case

maximum amplitude of the vibrations is designated by the peak, which is given by:

$$RMS = \sqrt{\int_{-\infty}^{\infty} x(t)^2 p(x) dx} \tag{3.2}$$

$$Peak = E \langle max[x(t)] \rangle \tag{3.3}$$

where, $x(t)$ is the random variable signal, $p(x)$ is the amplitude probability density function of $x(t)$ and E represents the expected value. RMS, which is an indicator of effective energy can be used to determine the condition of the bearing at any instant of time. The deterioration can be detected by the peak value changes. More information can be obtained from [4]. Gustafsson et al. determined the bearing condition by comparing the peak counts for the measured signal and for a signal with a Gaussian amplitude distribution. In the initial stages of the bearing fault, when the peaks have just begin to occur, discrete signals can be seen which keep the total vibration energy constant, and hence, the RMS remains virtually constant. There is an increase in the RMS only when the number of peak increases as a result of an increase in the fault level; but without much appreciable change in the level of the peak value. With the fault becoming more severe, both the RMS and Peak value increase, which can help in indicating the condition of the machine. Though RMS and Peak Values can be used to determine the energy levels of the fault signals obtained, yet, they cannot be used for single snapshot detection of the bearing damage, as the expected values generally exhibit wide range depending on the operating conditions such as the load and speed of the testing environment [4]. RMS and Peak values can be used effectively only unless the RMS and peak values are compared with the baseline values for the system, under the same operating conditions. Sun et al, proposed the usage of normalized RMS and peak values so that operation condition and non-defect induced vibration can be taken into consideration.

$$R_v = RMS/RMS_0$$

$$P_k = Peak/RMS_0$$

where, RMS_0 gives the reference value of a faultless bearing. This value can be obtained depending upon the application its being put into; in case of bearings in fixed machinery, RMS_0 could be the value taken under the loadless condition when the bearings are without any damage.

3.1.3 Statistical Parameters

Incipient faults can also be detected with the help of time domain statistical parameters. Some of the commonly used statistical parameters are: Histogram, Kurtosis Value, Crest Factor, covariance, correlation, and convolution.

Kurtosis Value

Kurtosis is a value which describes the shape of a random variable's probability density function. Figure 3.6 [20] shows some of the general forms of kurtosis. The PDF which is more peaked and which has flatter tails has higher kurtosis. The advantage of using kurtosis is that it's robust to the operating conditions.

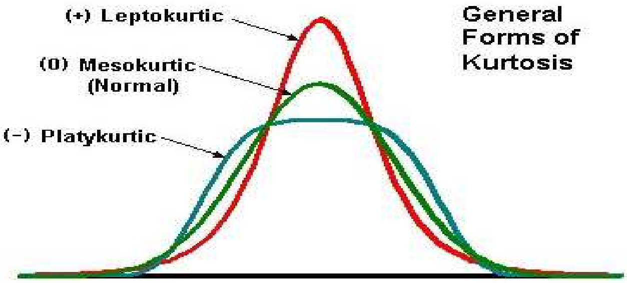

Figure 3.6 General Forms of Kurtosis

The kurtosis value is given by:

$$kv = \frac{\int_{-\infty}^{\infty} x(t)^4 p(x) dx}{[\int_{-\infty}^{\infty} x(t)^2 p(x) dx]^2} \tag{3.4}$$

where, $x(t)$ is the amplitude of the signal and $p(x)$ is the probability density function of the signal obtained from the machine. Kurtosis values of 4.0743, 6.074, 3.1197 (mechanical) and 1.5418 (electrical) are obtained for sample of data (figures 3.7 and 3.8) for the $20g$ applied to the middle of the disc for the mechanical test bed and for the faultless case for the electrical test bed respectively.

Crest Factor

It is the ratio of Peak and RMS value. It gives an indication of the spikiness of the signal obtained from the test system. It does not get affected with the changes in the bearing speed and load. Crest factor is partially effective in indicating bearing on-set defects as they tend to cause sharp impulses in the vibration signals [4]. An abrupt increase in Crest value can easily be observed. With the increase in

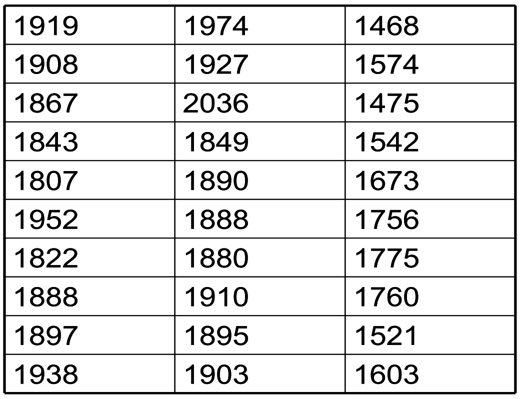

1919	1974	1468
1908	1927	1574
1867	2036	1475
1843	1849	1542
1807	1890	1673
1952	1888	1756
1822	1880	1775
1888	1910	1760
1897	1895	1521
1938	1903	1603

Figure 3.7 Data Sample for finding Kurtosis values-Mechanical test bed

damage, the number of impulses per cycle increases, which causes an increase in the value of the RMS keeping a constant peak value. The Crest factor which is given by equation 3.5 will decrease under these conditions.

$$cf = \frac{E\left\langle [x(t)] \right\rangle}{\sqrt{\int_{-\infty}^{\infty} x(t)^2 p(x) dx}} \tag{3.5}$$

The shape of probability density distribution can be known through a series of statistical moments, which are defined as follows:

$$M_n = \int_{-\infty}^{\infty} x_n p(x) dx \tag{3.6}$$

where, $n = 1, 2, 3, ..., m$ represents the order of the statistical moment and m is the maximum order under consideration. The first moment gives the *mean value*, where as the second moment gives the *standard deviation.* *Skewness* is given by the third moment and *kurtosis* is given by the fourth moment.

Both Kurtosis and Crest Factor respond only to the level of spikiness of the signal measured and are independent of the actual value of the signal.

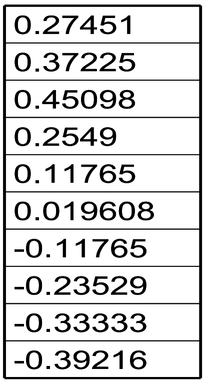

0.27451
0.37225
0.45098
0.2549
0.11765
0.019608
-0.11765
-0.23529
-0.33333
-0.39216

Figure 3.8 Data Sample for finding Kurtosis values-Electrical test bed

3.1.4 Covariance, Correlation and Convolution

Covariance

The covariance gives a measure of the extent to which two variables change together. Mathematically it is given by

$$P_x(n) = \frac{1}{N}\sum_{k=1}^{N}(x_k - x^{-})(x_{k+n} - x^{-}) \qquad (3.7)$$

where, x_k is the time series, N is the time interval.

The covariance between the two variables will be positive, if two variables tend to vary together (that is, when one of them is above its expected value, then the other variable tends to be above its expected value too), and its negative, if one of them is above its expected value and the other variable tends to be below its expected value. Details on this can be got from [2]. Figure 3.9 gives a sample of the three dimensional data (vibration sensor readings) from which covariance values as shown in figure 3.10 have been calculated.

Correlation

The correlation gives the strength and direction of a linear relationship between

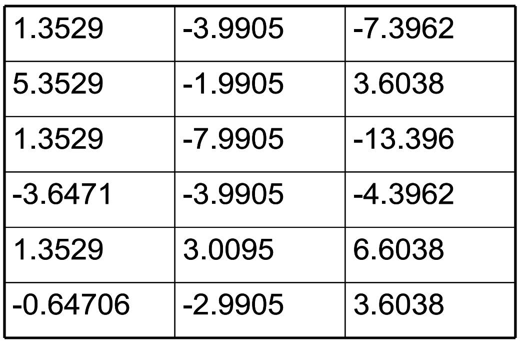

1.3529	-3.9905	-7.3962
5.3529	-1.9905	3.6038
1.3529	-7.9905	-13.396
-3.6471	-3.9905	-4.3962
1.3529	3.0095	6.6038
-0.64706	-2.9905	3.6038

Figure 3.9 Sensor/Data readings for computing the covariance values

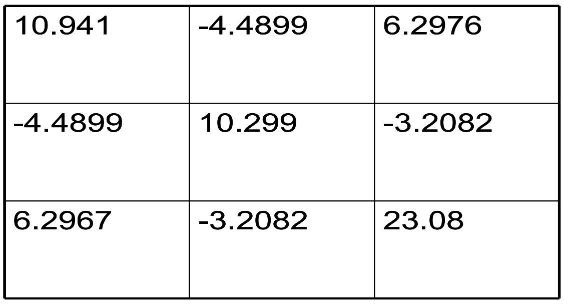

10.941	-4.4899	6.2976
-4.4899	10.299	-3.2082
6.2967	-3.2082	23.08

Figure 3.10 Covariance Values

two variables. It is called cross-correlation when it's been two vectors and is defined as:

$$R_{xy}(n) = \frac{1}{N}\sum_{k=1}^{N}(x_k y_{k+n}) \tag{3.8}$$

When the y is replaced by x in equation 3.8, we get *auto-correlation*. The correlation values can be seen from figure 3.11, which have been calculated from the data set (three dimensional values from the vibration sensor) recorded, a sample of which has been shown in figure 3.12.

The measure cross-covariance is given as

$$P_{xy}(n) = \frac{1}{N}\sum_{k=1}^{N}(x_k - x^{-})(y_{k+n} - y^{-}) \tag{3.9}$$

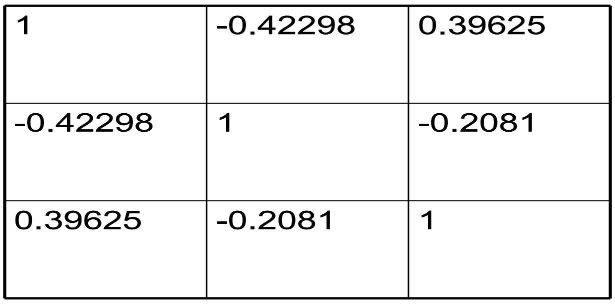

1	-0.42298	0.39625
-0.42298	1	-0.2081
0.39625	-0.2081	1

Figure 3.11 Correlation Values

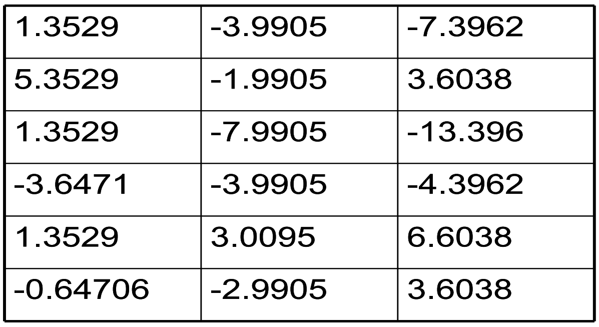

1.3529	-3.9905	-7.3962
5.3529	-1.9905	3.6038
1.3529	-7.9905	-13.396
-3.6471	-3.9905	-4.3962
1.3529	3.0095	6.6038
-0.64706	-2.9905	3.6038

Figure 3.12 Data to compute the correlation values

Convolution

Convolution is a mathematical operator that takes two functions and produces a third function, which is the modified version of one of the original function. It has applications in *signal processing*, *statistics* etc. The discrete-time convolution for N point sequence is given by:

$$x * y(n) = \sum_{k=0}^{N-1} x_k y_{n-k} \tag{3.10}$$

This actually gives the polynomial multiplication. Correlation can be expressed in terms of convolution as [2]:

$$R_{xy}(n) = \frac{1}{N}\sum_{k=1}^{N}(x_k y_{k+n}) = \frac{1}{N}x(k) * y(-k) \tag{3.11}$$

CHAPTER 4

INTRODUCTION TO FREQUENCY DOMAIN ANALYSIS

Analysis of any signal with respect to frequency is called “Frequency-Domain” Analysis. Major frequency components and their amplitudes are used for detecting short circuit current and bearing faults in an induction motor, which requires the fundamental frequency to be known beforehand. This chapter describes the various frequency domain techniques such as Power Spectral Density and Discrete Fourier Transform and also shows the outputs that were obtained when these methods were performed on the signals obtained from the motor under consideration.

4.1 Frequency Domain Analysis

Time domain analysis can be used to detect faults but, they cannot be used to determine the location of the fault (that is, whether the fault in the inner, middle or outer ring of the disc simulating the faulty bearing as in the case of mechanical fault) [6]. The frequency spectrum analysis of the time signal is done using discrete Fourier transform (DFT). The DFT is a specific form of Fourier analysis, which requires a discrete input whose non-zero values has a limited duration. Therefore, it is a transform for Fourier analysis of finite time domain discrete-time functions. *Fast Fourier Transform* (FFT) is an efficient algorithm to compute DFT. Given an N-point time series $(x(n))$, DFT is given by:

$$X(k) = \sum_{n=1}^{N} x(n) e^{j2\pi(k-1)(n-1)}/N \tag{4.1}$$

where, $k = 1, 2, 3, ..., N$.

The spectrum of the signal can be used for diagnosis of the faults. A fundamental frequency of $60Hz$ is used for all the analysis of the vibration spectra. The frequency spectrum under faultless and fault ($20mH$ inductance) condition for the electrical fault can be seen from figures 4.1 and 4.2 respectively. Figures 4.3 and 4.4 show the frequency spectrum under the faultless and fault condition($5g$ inner) for the mechanical test bed. Fast Fourier Transform has been performed on the signals recorded by the sensors in order to get the spectrum. We can see distinctive peaks (harmonics) in the plots in the case of the machine under fault as compared to the faultless condition. These peaks in the spectrum indicate the presence of faults.

The contact stress between the rollers and raceways are high, which

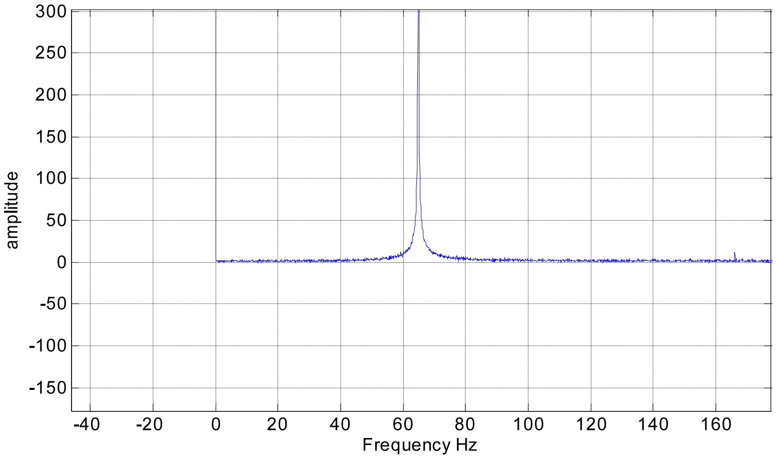

Figure 4.1 Frequency Spectrum for faultless condition-Electrical Test Bed

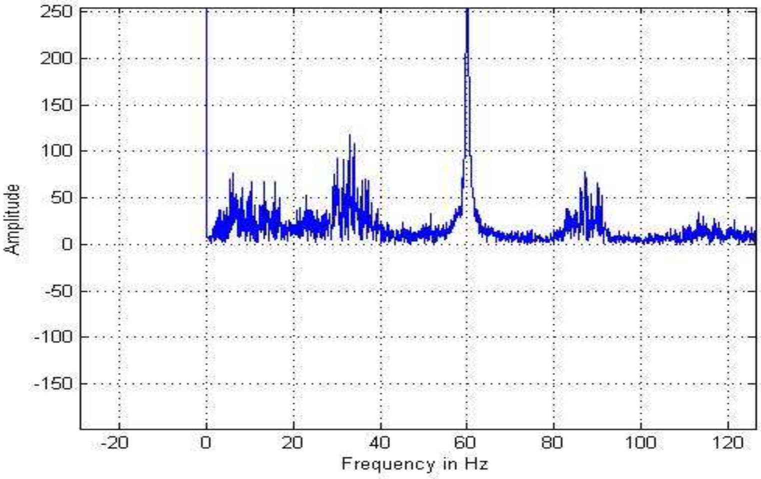

Figure 4.2 Frequency Spectrum for a fault condition-Electrical Test Bed

results in abrupt changes in the stress caused by the passage of defects; resulting in impulsive excitations to the structure. Details can be obtained from [4] and [8]. In the case of mechanical test bed, the weight can be placed on the inner, middle or outer ring of the disc. It is known that the vibrations produced are more in the case of weight being applied to the outer ring. Figures 4.5, 4.6 and 4.7 show the spectrum produced when a weight of $20g$ is added to the outer, middle and inner rings (simulating the faulted bearing) respectively. We can clearly see that the number of peaks are more in the case when the $20g$ weight is added to the outer ring than in the case when it is added to the inner ring, which implies that the vibration produced is more when the weight is placed in the outer ring rather than when it is placed in the inner ring. Similar results are obtained in the case of electrical fault as well when the fault has a resistance included in it compared to the case when it is a solid fault as shown in figures 4.8 and 4.9

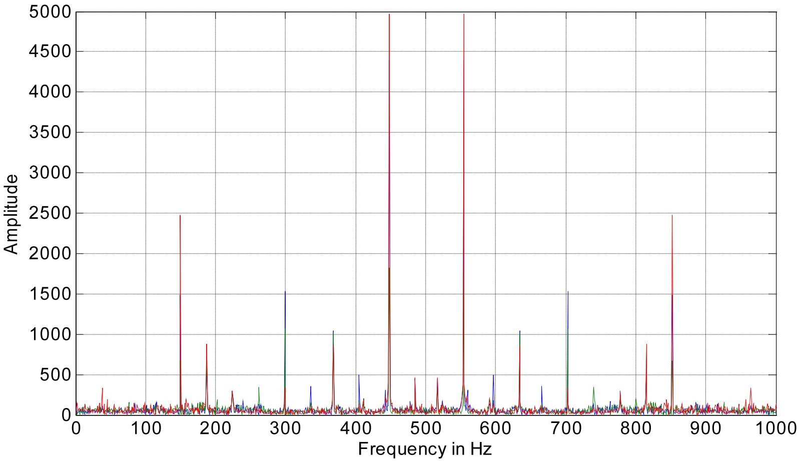

Figure 4.3 Frequency Spectrum for faultless condition-Mechanical Test Bed

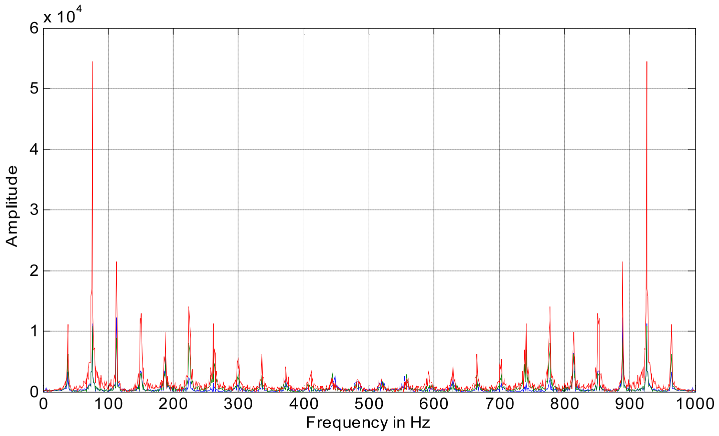

Figure 4.4 Frequency Spectrum for a fault condition-Mechanical Test Bed

Although, the frequency spectrum can be used to detect the position of the fault, yet it is difficult to automatically detect the impulses at these frequencies because the frequency spectrum shows stronger peaks at higher frequencies, representing higher order structural resonance compared to the characteristic frequencies. Vibration energy of the bearing which spreads across a wider bandwidth could easily get buried in the noise.

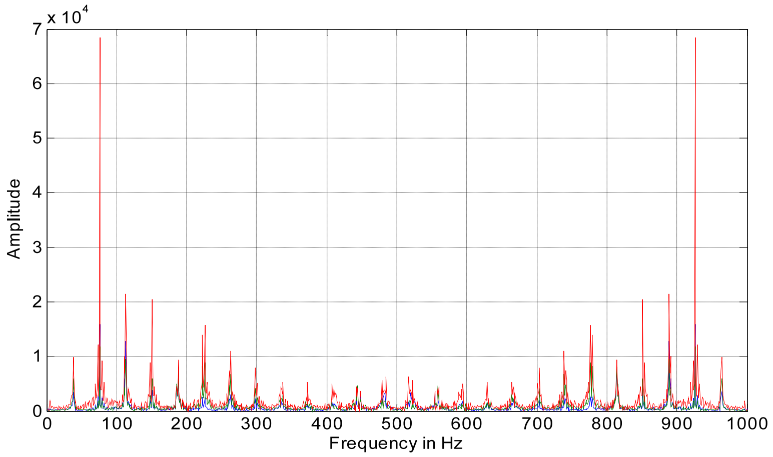

Figure 4.5 Frequency Spectrum of “20 g” weight in the outer ring

4.1.1 Properties of Discrete Fourier Transform

Details on the properties of DFT can be found in [2]. Some of the properties of DFT are:

- Parseval's Theorem:

  It can be mathematically stated as:

$$\sum_{n=1}^{N} x_2(n) = \frac{1}{N}\sum_{k=1}^{N} |X(k)|^2 \tag{4.2}$$

- Convolution Theorem:

  It states that the transform of the convolution

$$x * y(n) = \sum_{k=0}^{N-1} x_k y_{n-k} \tag{4.3}$$

  is given by the product of the transforms $X(k)Y(k)$. This actually means that the convolution in one domain (e.g., frequency domain) is equal to the point-wise multiplication in the other domain (e.g.,time domain)

- Correlation Theorem It states that the transform of the correlation

$$R_{xy}(n) = \frac{1}{N}\sum_{k=1}^{N}(X_k Y'(k+n)) \tag{4.4}$$

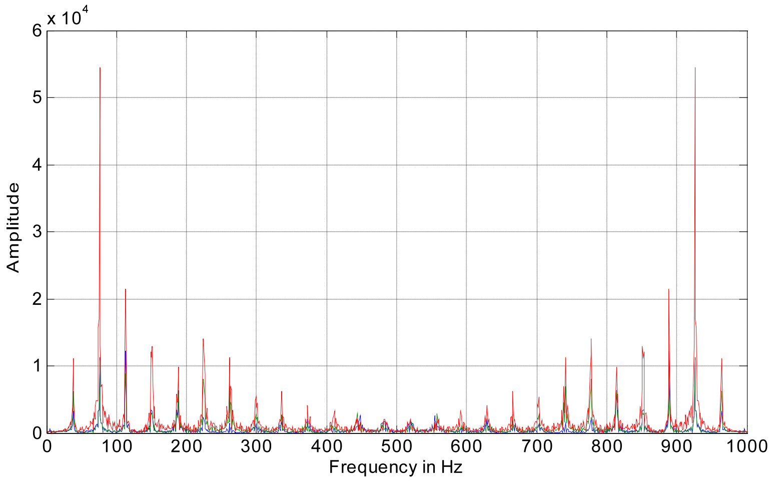

Figure 4.6 Frequency Spectrum of “20 g” weight in the middle ring

is given by $X(k)Y'(k)/N$, where, $Y'(k)$ denotes the complex conjugate transpose of $Y(k)$.

4.1.2 Power Spectral Density

Power Spectral density is a positive real function of a frequency variable associated with a stochastic stationary process, or a deterministic function of time. It captures the frequency content of the measured signal. It is mathematically defined as [2]

$$\Phi_k = \frac{1}{N}X(k)X'(k) = \frac{1}{N}|X(k)|^2 \tag{4.5}$$

Figure 4.10 shows the plot of power spectral density for the electrical test bed where an inductance of $20mH$ has been added to the middle of the coil.

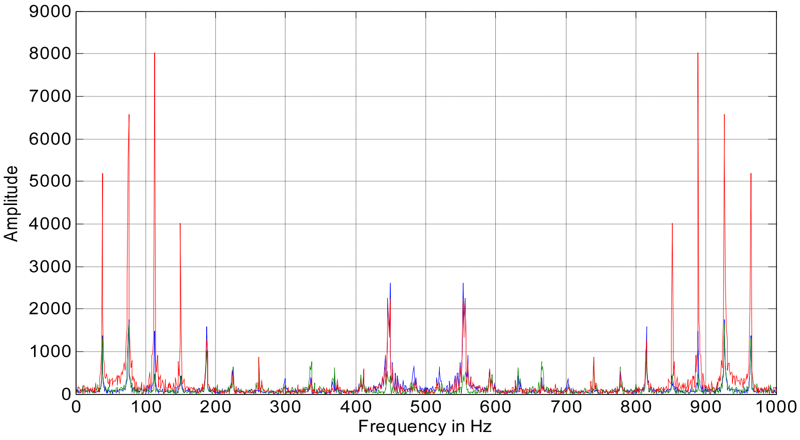

Figure 4.7 Frequency Spectrum of “20 g” weight in the inner ring

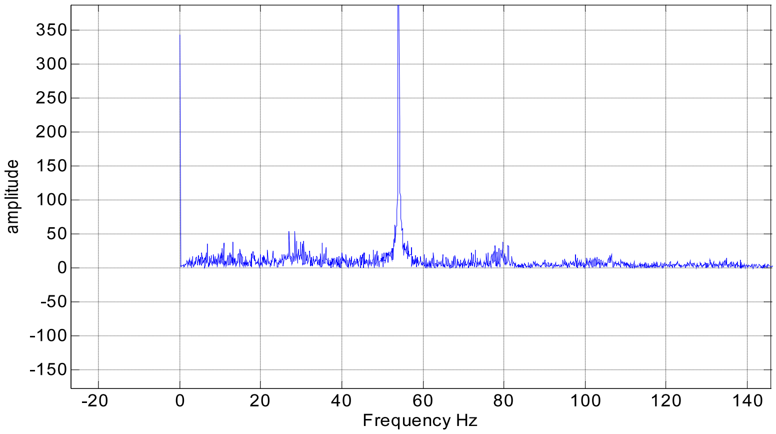

Figure 4.8 Frequency Spectrum of Solid Fault

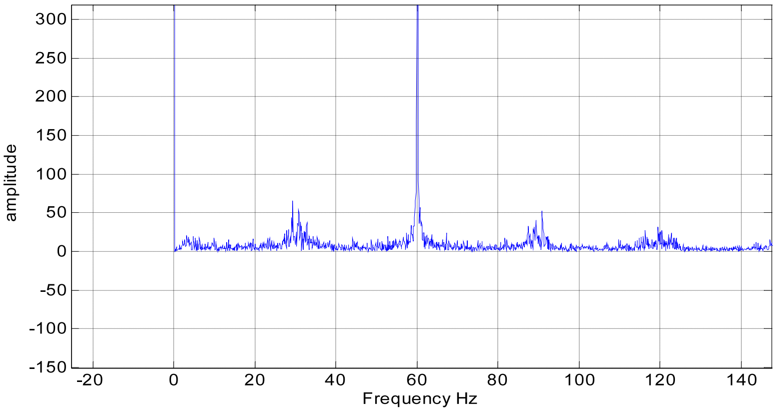

Figure 4.9 Frequency Spectrum of Resistance Fault

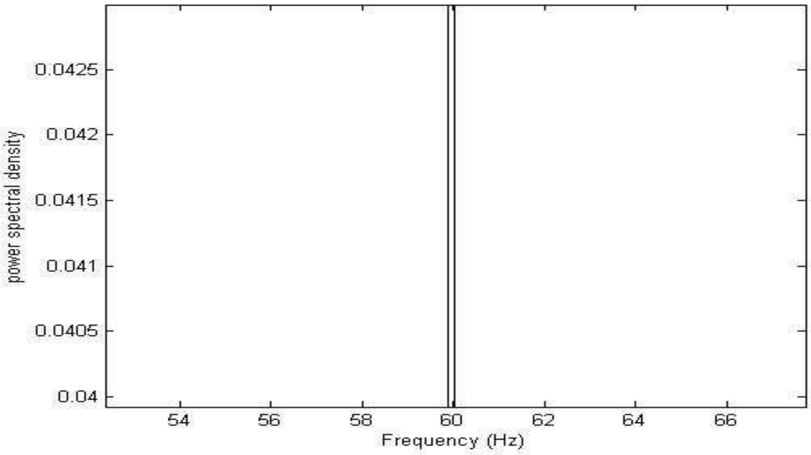

Figure 4.10 PSD of a $20mH$ inductance added to the middle of the coil

CHAPTER 5

TWO STAGE NEURAL NETWORK

The data collected from the wireless modules is analyzed using a two-stage neural network for “fault classification”. Reduction in dimensionality of the large amount of data recorded is one of the important steps before the data can be classified into various fault types. Therefore, this chapter describes a novel two stage neural network, where, the first stage is used for estimation of Principal Components and the second stage is used for fault classification.

5.1 First Stage Neural Network: Principal Components Estimation

Principal Component Analysis (PCA) is a vector space transform which is used to reduce the dimensionality of the large amount of the data recorded. PCA is a way of identifying patterns in a data, and expressing the data in a way so that it can highlight the differences and similarities [21]. Therefore, PCA becomes a powerful tool for analysis of data. This reduction is done by retaining only those values in the data set which have a significant value of variance. The main advantage of this method is that the information content is retained despite a reduction in the dimensionality. PCA is used for two reasons:

- to reduce the dimensionality of the data and
- to extract the features

Hebbian Learning Rule Neural Network is used for PCA estimation. Information on PCA estimation using GHA can be found in [22] and [21]. It is used because it extracts m actual principal eigenvectors as those obtained from the conventional method. PCA estimation consists of the following steps:

1. Finding the mean of the data set.
2. Subtracting the mean from each of the values in the data set. This produces a data set which has zero mean.
3. Calculating the covariance matrix.
4. Finding the eigenvalues and eigenvectors of the covariance matrix. The calculation of eigenvectors and eigenvalues of the covariance matrix helps in extraction of those lines which characterize the data. These eigenvectors which have been calculated are *unit* eigenvectors, i.e., their lengths are 1.
5. Arrangement of these eigenvectors in a descending order to get the components in the order of their significance. This would help in ignoring components with lesser significance and hence, bring about a reduction in the dimension of the data. For e.g., n original eigenvalues would be reduced to p values after the elimination of smaller values.
6. The feature vectors are then formed in the columns with the chosen eigenvectors. The matrix will look like this after its formulation:

   $$Featurevector = (eig_1 eig_2 eig_3 ... eig_n) \tag{5.1}$$

7. Deriving the new data set. This can be shown mathematically as:

   $$FinalData = RowFeatureVector \times RowDataAdjust \tag{5.2}$$

   where, $RowFeatureVector$ is the matrix with the eigenvectors in the columns transposed so that we now have the eigenvectors in the rows, and $RowDataAdjust$ is the mean-adjusted data transposed, i.e., the data items are in each column, with each row holding a separate dimension and $FinalData$ is the

> final data set, with data items in columns and dimensions along rows [21]. Through this transformation, the data is being expressed in terms of the patterns between them, which in turn describe the relationships between the data. This gives us the data values which tell the relation that it has with the rest of the data since our data is in terms of eigenvectors instead of the usual axes.

PCA compresses the data $X \epsilon R^{n\times 1}$ and gives a lower dimension of $y = WX$ where, $y = R^{m\times 1}$. Here, W matrix represents the eigenvectors chosen [23] [24] [25].

Neural Networks is preferred for PCA estimation rather than statistical methods because of its flexibility in terms of online adaptive reformulation [26]. The conventional method involves calculation of the covariance matrix and then application of the diagonalization procedure for extracting the eigenvalues and corresponding eigenvectors. As the size of the data increases, matrix manipulation and computation becomes cumbersome and inefficient due to round off errors. Hence, this poses a limitation on the statistical based methods [27].

Let us take an example in order to understand the difference between the 2 approaches: The dimension of the vibration data obtained is: $[XYZ]^T = [5, 10, 15]^T$ and the total number of data points is $M = 16000$. This data($[5, 10, 15]$) gives the vibration value in x, y and z directions respectively. The data points obtained are converted to one dimensional vector given by τ_i, corresponding to the data point i. The dimension of τ_i is $\{N, 1\}$, where, $N = X \times Y \times Z = 750$. The mean of the data set is given by:

$$\psi_i = \frac{1}{M} \sum \tau_k = \frac{1}{M}[\tau_1 + \tau_2 + ... + \tau_M] \tag{5.3}$$

And subtracting the mean from the original data gives the difference value as :

$$\phi_i = \tau_i - \psi \tag{5.4}$$

where, $i = 1, 2, 3, ..., M$. The difference values are gathered to form a set which is given by

$$A = [\phi_1 \phi_2 \phi_3 ... \phi_M] \tag{5.5}$$

where, the dimension of A is $[750, 16000]$. The covariance matrix C is obtained as

$$C = \frac{1}{M} \sum_{n=2}^{M} \phi_n \phi_n^T = AA^T \tag{5.6}$$

The eigenvectors of C are computed to form the transformation matrix W. It can be observed that the dimension of the matrix C is N, N which makes it cumbersome to compute the N eigenvectors. As the number of eigenvectors giving information about the data is equal to the number of data points over which the information is obtained; therefore, only M eigenvectors are used to form the W matrix. In order to compute the M eigenvectors the following method is used, where a new matrix is given as

$$L = AA^T \tag{5.7}$$

The dimension of L is $\{M, M\}$ and let its eigenvalues be μ_i and the eigenvectors be ρ_i.

Therefore we get

$$L\rho_i = \mu_i \rho_i \tag{5.8}$$

Substituting for L in equation 5.8, we get

$$A^T A \rho_i = \mu_i \rho_i \tag{5.9}$$

Multiplying the above equation 5.9 by A gives

$$AA^T A \rho_i = A \mu_i \rho_i \tag{5.10}$$

Since, $C = AA^T$, therefore, $A\rho_i$ are the eigenvectors of matrix C. This results in computation of M eigenvectors instead of N eigenvectors. Then the transformation matrix W is constructed for dimension reduction. From this we can observe that this approach requires all the information to be known in advance for formulating the transformation matrix W. The addition of new data would entail repetition of the entire process of PCA estimation. The use of neural networks tackles this problem by presenting only the new data to the Neural Network, hence avoiding batch processing.

The algorithm for estimating the PCA is the re-estimation algorithm in which the neural network has only forward connection, whose weights are modified following the *Generalized Hebbian Algorithm (GHA)* [22] [28]. The weight update equation is given by

$$w(n+1) = w(n) + \beta(n).y(n).(X - y(n).w(n)) \tag{5.11}$$

where, $w(.)$ is the synaptic weight vector connecting the input data vector, X, to the output, y. $\beta(n)$ is the learning-rate parameter. $\beta(n).y(n).X$ represents the Hebbian modification to $w(n)$. The negative term $-y(n).w(n)$ assures stability; it modifies the input X in a manner which is dependent on $y(n)$ (output) and $w(n)$ (synaptic weight). The $w(n)$ converges with probability 1 to the principal eigenvector of the covariance matrix of the input data . The generalization of this learning rule may be used to train a feedforward part of the network. The vector $w_j(n)$ is adapted using Sanger's and Oja's rule based on the GHA [29] [30] [25]as

$$w_j(n+1) = w_j(n) + \beta(n).y_f(n).(X' - y_f(n).w_f(n)) \tag{5.12}$$

$$X' = X - \sum_{k=1}^{j} w_k y_k \tag{5.13}$$

where, X' represents the modified input. The behavior of the feedforward network from equations 5.12 and 5.13 is as follows:

1. $j = 1$ and $X' = X$ for the first PC extraction. The GHA then gets reduced to equation 5.11, which causes convergence to the eigen vector with largest eigenvalue.

2. $j = 2$ and $X' = X - w_1.y_1$ for the second PC extraction, provided the first neuron has already converged to the first PC, which is y_1. The second neuron which sees an input X', therefore, extracts the first PC of X', which is equivalent to the second PC of the original input vector (i.e., second largest eigenvalue and associated eigenvector).
3. $j = 3$ and $X' = X - w_1.y_1 - w_2 y_2$, for the third PC extraction, provided the first two neurons have already converged to the first and the second PC respectively. The third neuron now sees the input vector X' from which the first two eigenvectors, w_1 and w_2 have been removed. It results in the extraction of the first PC of X', which is equivalent to the third PC (i.e., the third largest eigenvalue and associated eigenvector) of the original input vector X.
4. The process continues like this till the output for each of the hidden layers is got as shown in figure 5.1 which eventually results in the extraction of all the Principal Components.

This phase is followed by the second phase where, the synaptic weight vectors of the neurons in the feedforward part of Figure 5.1 [28] converge to the normalized eigenvectors associated with the largest P eigenvalues of Σ_X, ordered in descending order [28]. Therefore, we get $\delta w_j(n) \to 0$ and $w_j(n) \to u_j$ as $n \to \infty$, with $\|w_j(n)\| = 1$, for all j. This can also be written as: $lim_{asn\to\infty} y_j(n) = X^T.u_j = u_T.X$, which means

$$lim_{x\to\infty} E(y_j(n).y_k(n)) = u_T.\sum_X .u_K = \{\lambda_j, k = j\} \tag{5.14}$$

$$lim_{asn\to\infty} E(y_j(n).y_k(n)) = u_T.\sum_X .u_K = \{0, k \neq j\} \tag{5.15}$$

where, $\hat{X}$ is the reconstructed input vector X for which equations 5.14 and 5.15 is satisfied for $j = P$. Therefore, we get

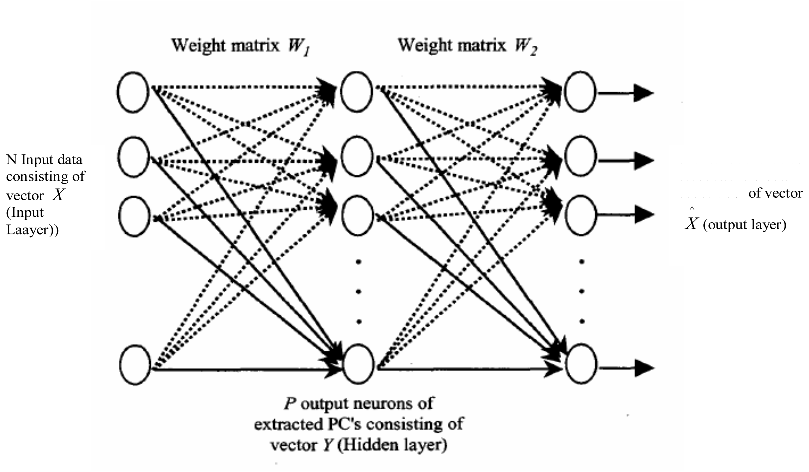
Weight matrix W_1
Weight matrix W_2
N Input data consisting of vector X (Input Laayer))
of vector $\hat{X}$ (output layer)
P output neurons of extracted PC's consisting of vector Y (Hidden layer)

Figure 5.1 PCA Neural Network Model for Principal Component Extraction

$$\hat{X} = \sum_{k=1}^{P} y_k(n).u_k \text{ as } n \to \infty$$

W_1 and W_2 correspond to the optimal weight matrices of the two parts of the network as shown in the figure 5.1. The relationship between W_1 and W_2 can be defined as $W_2 = W_1^T$, where W_1 is a matrix with rows consisting of the P normalized principal eigenvectors of Σ_x. Because of this constraint, the weight vectors have unit norm. The aim now becomes combining the two parts of the vector to, develop a training algorithm to extract all the Principal Components. It becomes necessary to develop a function that would drive the weight vectors towards the normalized eigenvectors associated with the eigenvalues of Σ_x, and to provide an optimal data reconstitution at the outputs of the second layer. Let w_j be the synaptic vector of the first matrix, W_1, while w_j^T is the synaptic weight of the second matrix W_1^T. Let also assume that the neurons are trained sequentially, therefore, the extraction of every PC differs from the others. $y_1(n+1) = w_1^T(n).X$ gives the output of the first hidden layer at iteration n, and $\hat{X} = w_1(n).w_1^T(n).X$ is the output of the network. At mth iteration, the criterion for first PC extraction becomes $C_m = \sum_{n=1}^{m}(X - \hat{X})^T(X - \hat{X})$. From equations 5.12, 5.13 and 5.1, by taking the partial derivative of C_1 according to $\hat{w}_1(n)$ and setting it to zero, we get

$$\sum_{n=1}^{m} y_1(n).(X - \hat{w}_1(m).y_1(n)) = 0 \tag{5.16}$$

The equation 5.16 which gives the performance criterion should be tend to zero when the synaptic weight converges to the principal eigenvector of $\sum_X$ [28]. The deflated data is used for extraction of the other Principal Components. Hence, the objective function that is to be used for each PC extraction is :

$$\sum_{n=1}^{m} y_j(n).(X - \hat{w}_j(m).y_j(n)) = 0 \tag{5.17}$$

where, j gives the neuron order. The equation 5.17 should be nearing zero, at convergence, which means that the synaptic weight vector (w_j) converges to the eigenvector of Σ_X.

5.1.1 Convergence Rate

The convergence rate for the PC extraction as mentioned in section 5.1 depends on the value of the *learning rate parameter*$(\beta(n))$, and the manner in which its value gets computed during the learning process. The learning rate parameter is also dependent on the statistical characteristics of the input data because of which the updating process becomes self-regulatory, bringing about improved convergence characteristics in terms of both speed and accuracy. Accuracy versus convergence speed trade-off problems are mentioned in [26] and [30]. It also gives a good method to find the variance associated with each PC recursively. The learning-rate parameter for each neuron j, at iteration n is given as

$$\beta_j(n+1) = P_j(n).y_j(n+1)/(1+y_j^2(n+1).P_j(n)) \tag{5.18}$$

$$p_j(n) = (\sum_{l=1}^{n} y_j^2(l))^{-1} \tag{5.19}$$

The variance of the output neuron can be found out directly without finding them out from the neuron output. The variance can be computed as follows:

$$(P_j((n+1).L)^{-1} - P_j(n.L)^{-1}) = \sum_{k=n.M}^{(1+n).M} y_j^2(k) = \hat{\lambda}_j \tag{5.20}$$

where, L is the input data size.

5.1.2 Extraction of the Principal Components

5.1.2.1 First Principal Component

The structure for extraction of the Principal Components consists of a hidden layer with two neurons in it. The weight vector can be updated with the following algorithm [28]:

1. Initializing the weight vector $w_1(0)$ with some random value, and having $P_1(0) = 0.1$.
2. The output hidden neuron is given as $y_1(n+1) = w_1^T(n).X$
3. The weight vector gets updated as per the equations 5.11, 5.18 and 5.19
4. Evaluation of the performance criterion as given in equation5.16
5. Steps from 2 have to be repeated in the event of non minimization, else, the variance from equation 5.20 is computed.

5.1.2.2 Other Principal Components

The following steps are adopted for the other principal component extraction:

1. The weight vector is initialized with some small random value as in the previous case.
2. The new input data vector is formulated from equation 5.13.
3. Output hidden neuron is computed as in the previous case.
4. The weight vector gets updated as per the equations 5.12, 5.18 and 5.19.
5. Evaluation of the performance criterion as given in equation 5.16.
6. Steps from 2 have to be repeated in the event of non-minimization, else, the variance given by equation 5.20 is computed.

5.1.3 Independent Component Analysis(ICA)

Independent Component Analysis is a statistical and computational technique for revealing hidden factors that underlie sets of random variables, measurements or signals [31]. It is one of the methods for extracting useful information from data, where, statistically independent signals can be extracted from a mixture of signals. ICA gives a model, where, the data variables are assumed to be linear mixtures of some unknown latent variables, which in turn are assumed to be non-Gaussian and mutually independent of the observed data. ICA is based on the assumption that the components are statistically independent. If the signals are statistically independent, then each of the signals extracted by ICA will have been generated by different physical process, and will therefore be the desired signal [32].

ICA is related to conventional methods like the Principal Component Analysis.

ICA finds a set of independent signal sources, where as PCA finds a set of signals which have properties much weaker than Independent components, because incase of PCA, the components are *uncorrelated* with each other. For e.g., in case of a mixture of signals from the microphone, PCA would simply extract a set of uncorrelated signals from this, where as, ICA would extract a set of independent signals so that the extracted signals would be a set of signal.

Certain algorithms like *centering*, *whitening*, and *dimensionality reduction* are used for preprocessing the mixture of signals in order to reduce the complexity of the signals for future processing. Mathematically, Linear Independent Component Analysis can be divided into noiseless and noisy cases. Let the data be represented as a random vector $x = (x_1, x_2, ..., x_m)$ and the components be described as $s = (s_1, s_2, ..., s_n)$. The linear static transformation (W) into maximally independent components s measured by some function $F(s_1, s_2, ..., s_n)$ is described as:

$$s = Wx \tag{5.21}$$

5.1.3.1 Limitations Of Principal Component Analysis

1. The fact that Principal Component Analysis is a *non-parametric* analysis can be viewed as a strength as well as a weakness. Non-parametric methods are so called because they do not rely on the estimation of parameters such as the mean or the standard deviation. They are so developed because there is no prior information about the parameters of variable of interest in the data set. PCA is an optimal linear scheme which gives a unique answer, independent of any hypothesis about data probability. The assumption that *the system is linear* means that there are no coefficients that need to be adjusted based on user experience to get the output, hence, giving an output independent

of the user. This becomes a weakness-if one has *apriori* information of some of the features of the system, then a *parametric* estimation can be used. Methods such as *kernel PCA* are being used to in order to overcome the problem of linearity.

2. PCA makes use of eigenvectors and covariance matrix and finds the independent axes of the data under the Gaussian assumption. In case of non-Gaussian data, PCA de-correlates the axes. When used for clustering, PCA does not account for class separability, as it makes no use of the class label of the feature vector. The directions of maximum variance may not contain good features for discrimination.

3. PCA assumes that large variances have important dynamics; this is true only when the observed data has a high signal-to-noise ratio. PCA just performs a coordinate rotation that aligns the transformed axes in the directions of maximum variance.

   Let us take an example where we are considering the position of a person on the Ferris wheel as shown in figure 5.2 [33]. (p_1, p_2) gives the extracted principal components and $\hat{\theta}$ gives the phase. The probability distributions along the axes are approximately Gaussian and thus, PCA finds (p1, p2), which may not be optimal. The best way to tackle this problem would be to find the phase or angle along the ferris wheel which may contain all dynamic information. Thus, the appropriate parametric algorithm is to first convert the data to centered polar coordinates and then compute the PCA [33]. This prior *non-linear* transformation is called *kernel transformation.* Even *Fourier* or *Gaussian* transformations can be used. This procedure is parametric because the user must incorporate prior knowledge of the structure in the selection of the kernel but it is also more optimal in the sense that the structure is more concisely described [33].

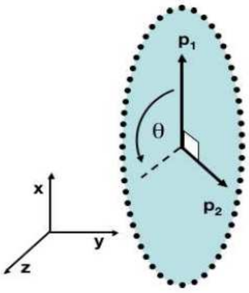

Figure 5.2 Data Points Tracking a person on the Ferris Wheel

5.2 Second Stage Neural Network

The second stage is used to classify the input data where the output of the first stage becomes the input to the second stage. This process is called *discriminative learning* which uses a supervised learning vector quantization (LVQ) network utilizing a self organizing map approach. Details on this can be obtained from [27] [22] [34]. It uses a training vector to distinguish the different categories of the input and is based on *winner-take-all* policy. This is preferred over Radial Basis Function or the Backpropagation method because the processing time is very less. The training of the network in supervised LVQ is done using standard Kohonen learning rule. The LVQ network consists of a first stage of competitive layer followed by a second stage of linear layer as shown in Figure 5.3.

The output of the first layer is given as:

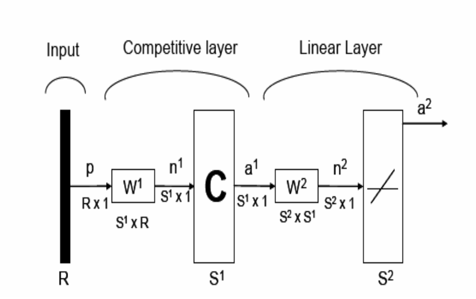

Figure 5.3 LVQ Network

$$a^1 = compet(\|w^1 - p)\| \tag{5.22}$$

where, p is the inputs with dimensions of $R \times 1$ elements and w^1 are the weights of the first layer of neural network. The second layer output is given as:

$$a^2 = W^2 a^1 \tag{5.23}$$

The number of neurons in equation 5.23 is S^2, which is equal to the number of classes; W^2 are the weights of the second layer of neural network. Therefore, the neurons with weight vector closest to the input vector will give an output as 1, and the other neurons will give an output as 0.

In the LVQ network, each neuron in the first layer is assigned to a class with many neurons being assigned to that class and each class is then assigned to a neuron in the second layer. The number of neurons in the first layer will therefore always be at least as large as the number of neurons in the second layer. As in the case of competitive network, each neuron in the first layer of the network learns a prototype vector allowing it to classify the inputs. Here, the LVQ vector is simulated using the distance directly rather than using the inner product between the weight vector and the input. This is advantageous, as the vectors need not be normalized; the response of the network is the same in either case when the vectors are normalized.

5.2.1 Self-Organizing Map(SOM)

SOM is used to transform an incoming signal pattern of arbitrary dimension into a one or two dimensional discrete map [26]. This is done adaptively in a topologically ordered fashion. Details on SOM can be obtained from [26]. The algorithm for SOM starts with initialization of the synaptic weights in the network. In doing so no prior order is imposed on the feature maps. This is followed by these three steps:

1. Competition: The neurons compute the discriminant function values in the input pattern, which forms the basis for competition amongst the neurons. The neuron with the largest value of discriminant function is declared the winner.
2. Cooperation: The winning neuron determines the spatial location of a topological neighborhood of excited neurons, thereby, providing the basis for cooperation among the neighborhood neurons [26].
3. Synaptic Adaptation: This lets the excited neurons to increase their individual values of the discriminant function with respect to the input though adjustments in the synaptic weights. This enhances the response of the winning neuron to the subsequent application of a similar input pattern.

5.2.2 Learning Vector Quantization(LVQ)

LVQ is a method of data compression by exploiting the underlying structure of the input vectors. The input space is divided into a number of regions and for each region, a reconstruction vector is is defined [26]. Upon being presented by a new input vector, the quantizer first determines the region in which the vector lies then the input is represented by the reproduction vector for that region. This encoded version for storage and transmission results in considerable saving in the storage or transmission bandwidth, though this happens with little distortion. A vector quantizer with minimum encoding distortion is called *Voronoi* vector.

LVQ is a supervised learning technique where class information is used to move the Voronoi vectors a little, so that the there is an improvement in the quality of the classifier decision regions. An input vector x is picked at random from the input space [26]. If the class labels of this vector and the Voronoi vector w agree, then the Voronoi vector is moved in the direction of the input vector, else moved away from the input vector.

CHAPTER 6

CLASSIFICATION OF FEATURE VECTORS

This chapter describes some of the classification and diagnosis techniques such as Fuzzy logic and Wavelet technique which can also be used for Condition Based Maintenance.

6.1 Classification

A classifier maps a list of measured features into a classification state. The aim of classification is to assign the input cases to one of a number of classes. More details on this can be obtained from [35]. Neural networks are categorized in accordance to the training algorithms as

- Fixed-Weights networks
- Unsupervised networks
- Supervised networks

Supervised Learning Rules

In this, the training data consists of many pairs of input/output patterns, where a teacher tells the output what its desired response to the input signals ought to be. Details on this can be found from [36]. Some of the examples in supervised learning are: error-correction learning, reinforcement learning, and stochastic learning. This type of learning suffers from the problem of error convergence (minimization of error between the desired and calculated values). Least Mean Square Convergence algorithm is used to compute the weights which minimize the error.

Unsupervised Learning Rules

In case of an unsupervised learning rule, the training set consists of input patterns only. The network trains to adapt depending on the experience through the previous training patterns; all in the absence of a teacher. Some of the examples of the unsupervised network are: Hebbian learning rule, and the competitive learning rule.

6.1.1 Different Techniques of Fault Classification

6.1.1.1 Wavelet Transform

A wavelet transform is a transform which provides time and frequency domain information simultaneously and hence, gives the time-frequency representation of the signal [37]. The signal-cutting problem is avoided in wavelet analysis because it uses a fully scalable modulated window. The window is shifted along the signal and for every position the spectrum is calculated [37]. This is followed by the repetition of the process with a slightly shorter (or longer) window for every new cycle. The end result would be a collection of time-frequency representations of the signal, all with different resolutions. This gives a multi-resolution analysis, and hence, a wavelet transform overcomes the shortcomings of a Fourier Transform. A wavelet is a waveform of limited duration with an average value of zero which can be described mathematically as

$$\int_{-\infty}^{\infty} f\left(t\right) \Psi\left(t\right) dt = 0 \tag{6.1}$$

Wavelet Analysis is a technique in which an array of N numbers is transformed from an array of N actual numerical values to an array of N wavelet coefficients. It is the decomposition of a signal into shifted and scaled versions of the mother wavelet, which in turn are formed by the translation of the a prototype function.

Details can be obtained from [38]. Each of the wavelet coefficients represents correlation between the wavelet function at a particular size and a particular location within the data array. By varying the size of the wavelet function (generally in powers-of-two) and by shifting the wavelet so that it covers the entire array, an overall match between the wavelet function and the data array can be built up. Wavelet functions are composed of a family of wavelet basis functions as shown in figure 6.1 [39]. The choice of a particular basis function depends on the application. Generally functions other than sine and cosine are chosen as these two are used for Fourier analysis.

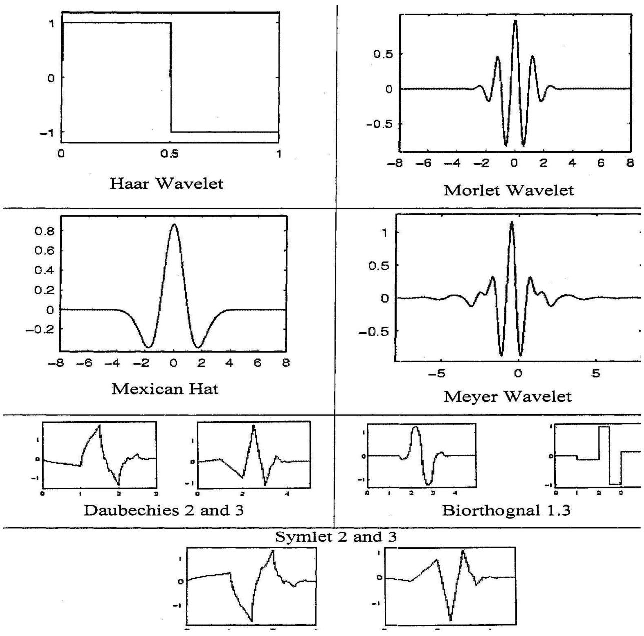

Figure 6.1 Some Basis Functions in Wavelet Analysis

Because of the compactness of the wavelet function, the wavelet coefficients measure the variations only around a small region of the data array, which makes it advantageous to be used in signal and image processing fields. The *localized* nature of the wavelet helps in feature extraction such as spikes (e.g., noise), edges of objects and discrete objects (e.g., satellite pictures) etc. Because of the localization, a wavelet coefficient at one location is not affected by the coefficients at another location in the data, thus, removing "noise" of all different scales from a signal by discarding the lowest wavelet coefficients. One of the main drawbacks of Fourier analysis is that it transforms signals in the frequency domain, where, the spatial distribution of the signal is not available. The wavelet transform overcomes this by retaining both the time and frequency domain information by decomposing the signal to multiple scales or resolutions. More details on this can be found in [40], [41], [42]. In wavelet transform, a real valued continuous time function is taken with two main properties: a) It will integrate to zero, and b) it is square integrable. This function is called the mother wavelet or wavelet (Ψ(t)). Property a) suggests that the function is oscillatory or wavy, and thus, in contrast to a sinusoidal function, it is a small wave or wavelet. Property b) suggests that most of the energy of the wave is confined to a finite interval. The continuous wavelet transform (CWT) of a function f(t) with respect to (Ψ(t)) is given as

$$W\left(a,b\right)=\int_{-\infty}^{\infty}f\left(t\right)\Psi_{a,b}^{*}\left(t\right)dt \tag{6.2}$$

where

$$\Psi_{a,b}\left(t\right)=\frac{1}{\sqrt{|a|}}\Psi\left(\frac{t-b}{a}\right) \tag{6.3}$$

a, b indicates the real parts where as * indicates conjugate. $W\left(a,b\right)$ is the transform coefficient of $f(t)$ for given a, b. Thus, the wavelet transform becomes a function of 2 variables. b represents time shift and a represents time scaling. If $a > 1$, then there is stretching of (Ψ(t)) along the time axis, where as, if $0 < a < 1$, then there is contraction of (Ψ(t)). Each wavelet coefficient $W\left(a,b\right)$ represents the measure of approximation of the input waveform in terms of the stretched and contracted versions of the mother wavelet. In order to reduce the computational burden, Discrete Wavelet Transform (DWT) is used. Though both CWT and DWT give time and frequency domain information using discrete sequences, yet, there is a difference between the two in the form of its output- DWT has several filters as the output, whereas, CWT has series of convolutions for every time shift. The fault detection using Wavelet Transform consists of comparing the current signature between the faulty condition and the faultless condition. One of the possible drawbacks of wavelet analysis could be lack in resolution in the higher frequency region. Hence, it could be a problem when analyzing signals in the high frequency region. Figure 6.2 shows the block diagram of the wavelet transform technique.

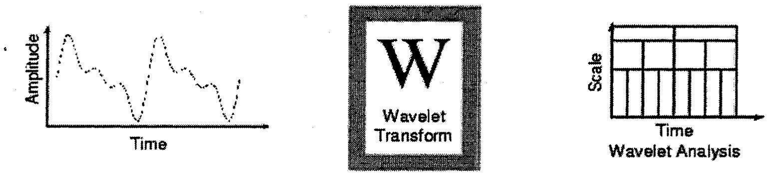

Figure 6.2 Wavelet Transform

6.1.1.2 Fuzzy Logic

The data collected by the sensors in motor fault diagnosis have to be interpreted and analyzed for which fuzzy logic can be used. Fuzzy logic is a multi-valued logic derived from fuzzy set for approximate reasoning. In fuzzy logic, the degree of truth of a statement can range between 0 and 1 and need not be restricted to

0 or 1 only. Details on CBM using Fuzzy logic can be found in [43], [44], [45], [46] and [47]. With the help of Fuzzy logic an item can be described as having a certain membership degree in a set. This allows a computer, which is normally constrained to 1 and 0, to delve into the continuous realm [48]. During induction motor fault diagnosis, there may arise situations where the fault may fall into some range which cannot be categorized as “good” or “bad”. Since fuzzy logic mimics human thinking, it can be used for fault diagnosis from vague information. By integrating human knowledge and experience Fuzzy sets and Fuzzy rules (which are obtained from the amplitude features of the stator current) can be defined for diagnosis. These rules and sets which help in the formulation of the knowledge database lead to the fuzzy inference. The induction motor condition can then be diagnosed using a compositional rule of fuzzy inference. The experimental set up could include measuring the stator current amplitude (I_a, I_b, I_c) as explained in [47]. As already mentioned, fuzzy systems rely on a set of rules which allow the input data to be *fuzzy.* Human interpretations like “overloaded” or “somewhat secure” can be expressed by the fuzzy system directly. This, therefore, eases the interface between domain knowledge and engineer knowledge and finally lets us simulate the real world where nothing can be concluded “concrete”. The fuzzy logic data recorded is represented in terms of linguistic information. The stator condition CM is chosen as the output where I_a, I_b and I_c are the inputs. These inputs and outputs are expressed in fuzzy set theory.

$$I_a = \mu_{I_a}(i_{aj})/i_{aj} \epsilon I_a$$

$$I_b = \mu_{I_b}(i_{bj})/i_{aj} \epsilon I_b$$

$$I_c = \mu_{I_c}(i_{cj})/i_{cj} \epsilon I_c$$

$$CM = \mu_{CM}(cm_j)/cm_j \epsilon CM$$

where, i_{aj}, i_{bj}, i_{cj}, and CM are the elements of discrete universe for the discourse I_a, I_b and I_c and CM respectively. $\mu_{I_a}(i_{aj})$, $\mu_{I_b}(i_{bj})$, $\mu_{I_c}(i_{cj})$, $\mu_{CM}(cm_j)$, are the corresponding membership functions respectively. Linguistic variables are values in an artificial language which provide a means of systematic manipulation of vague concepts. It is characterized by a quintuple $(x, T(x), U, G, M)$,where x is the variable name; $T(x)$ is the set of names of the linguistic values of x, each a fuzzy variable, denoted by x and ranging over a universe of discourse U. G is a syntactic rule for generating the names of x values; M is the semantic rule associating a meaning with each value. Details can be found from [47]. As an example, the term $T(CM)$ which gives the stator condition, CM, as a linguistic variable, can be $T(CM) = Good, Damage, SeriouslyDamaged$ where, each term of $T(CM)$ is characterized by a fuzzy subset in a universe of discourse CM. Good could be interpreted as a stator with no faults, damaged as a stator with voltage unbalance, and seriously damaged as a stator with an open phase. The stator condition as a linguistic variable is shown in figures 6.3 [47].

Similarly, the input variables I_a, I_b, and I_c are interpreted as linguistic variables, with

$$T(Q) = Zero, Small, Medium, Big \tag{6.4}$$

Where $Q = Ia, Ib, Ic$ respectively. The data set is observed to build the fuzzy rules and membership functions. The membership functions for the stator currents will be generated for zero, small, medium and big. As far as the measurement for stator condition is concerned, it is only necessary to know whether the stator is in *good, damaged or seriously damaged condition.* Figure 6.4(Z: Zero, S: Small, M: Medium, and B:Big) [47] and figure 6.5(G: Good, D: Damaged, and SD: Seriously Damaged) [47] show the membership functions for the stator currents

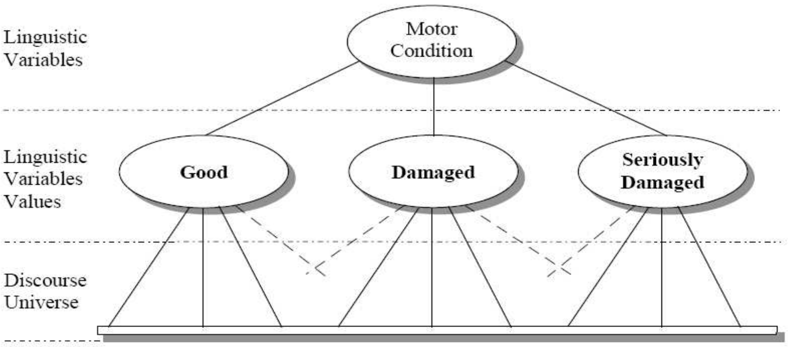

Figure 6.3 Linguistic Variables denoting Induction motor Stator condition

and condition respectively. After the determination of the membership functions, the fuzzy *if-then* rules are derived. Some of the fuzzy rules for stator voltage imbalance and open voltages are:

- Rule 1: If I_a is Z then CM is SD
- Rule 2: If I_b is Z then CM is SD
- Rule 3: If I_c is Z Then CM is SD
- Rule 4: If I_a is B Then CM is SD
- Rule 5: If I_b is B Then CM is SD
- Rule 6: If I_c is B Then CM is SD
- Rule 7: If I_a is S and I_b is S and I_c is M Then CM is D
- Rule 8 : If I_a is S and I_b is M and I_c is M Then CM is D
- Rule 9 : If I_a is M and I_b is S and I_c is M Then CM is D
- Rule 10 : If I_a is M and I_b is M and I_c is M Then CM is G

- Rule 11 : If I_a is S and I_b is S and I_c is S Then CM is G
- Rule 12 : If I_a is S and I_b is M and I_c is S Then CM is D
- Rule 13 : If $I_a$is M and I_b is S and I_c is S Then CM is D
- Rule 14 : If I_a is M and I_b is M and I_c is S Then CM is D

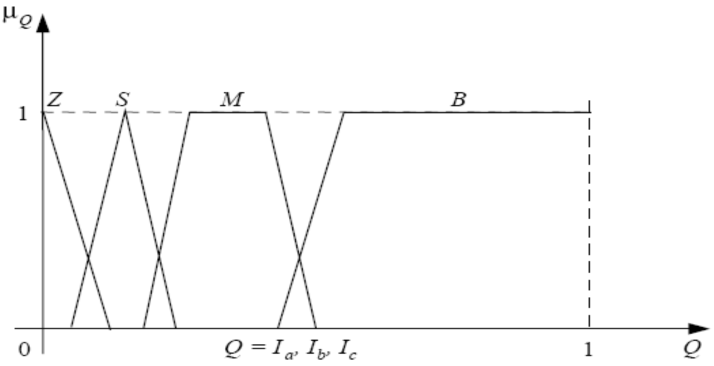

Figure 6.4 Fuzzy membership function for the stator currents

For diagnosis, the amplitudes measured were converted to corresponding discourse universe as inputs. The inputs are then evaluated by the fuzzy logic inference engine using the knowledge base. The ultimate step consists of converting the fuzzy action into "net results".

6.1.1.3 Hidden Markov Model

A finite state Hidden Markov Model consists of a finite number of states. A detailed explanation of Markov Models is provided in [49] [6]. Transition probabilities govern the transitions between the various states. Markov Models are used in places where the occurrence of an event depends on the previous events.

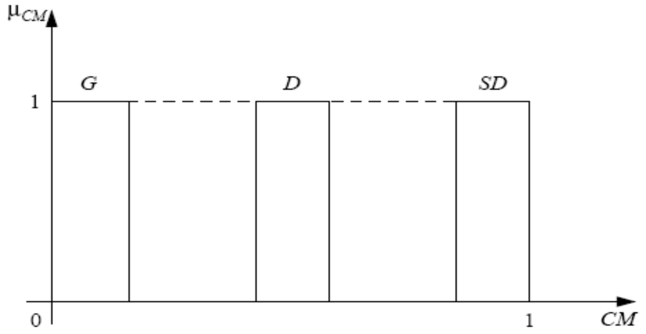

Figure 6.5 Fuzzy membership function for the stator condition

Hidden Markov Models are Markov models where the observations become the probabilistic functions of the state rather than the states themselves. Its so called because the underlying stochastic processes, state sequences are hidden and can be estimated only from another set of stochastic processes that produce the same sequence of observation. Some of the types of HMM are: *ergodic model* and *parallel path left-to-right model* etc.

The figure 6.6 [6] below shows the left-to-right HMM. The elements required for HMM:

- Number of states, N
- The transition probability, $A = a_{ij}$ where

$$a_{ij} = p\{q_{t+1} = j|q_t = i\},\ 1 \leq i,\ j \leq N,$$

where, q_t denotes the current state.

This gives the probability of being in state j at $t + 1$ provided the state

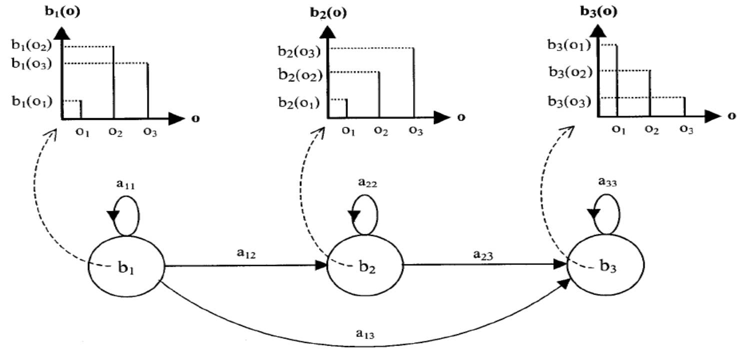

Figure 6.6 Three state left-to-right Hidden Markov Model

at time t is i. For a stochastic matrix A, the following conditions must be satisfied:

$$a_{ij} \geq 0,\ 1 \leq i,\ j \leq N\ \sum_{j=1}^{N} = 1,\ 1 \leq i,\ j \leq N$$

Since in the case of left-to-right HMM, the transitions are uni-directional, the matrix A is upper-triangular.

- Observation probability distribution of each state, $B = b_j(k)$, where

$$b_j(k) = po_k|q_t = j,\ 1 \leq j \leq N,\ 1 \leq k \leq M$$

$$o_k = k^{th} \text{ observation}$$

$$M = \text{number of distinct observation}$$

These conditions must be satisfied:

$$b_j(k) \geq 0,\ 1 \leq j \leq N,\ 1 \leq k \leq M$$

$$\sum_{k=1}^{M} b_j(k) = 1,\ 1 \leq j \leq N$$

i.e, the discrete probability should be positive and must sum up to one for each state. A continuous probability density function for each state must be specified for a continuous observation, in which case a weighted sum of several Gaussian distributions is used.

$$b_j(o_t) = \sum_{m=1}^{M} c_{jm} N(\mu_{jm},\, \Sigma_{jm},\, o_t), \text{ where } c_{jm} = \text{weighter coefficients}$$

$$\mu_{jm} = \text{mean vectors}$$

$$\Sigma_{jm} = \text{covariance matrices}$$

$$o_t = t^{th} \text{ observation vector}$$

where, the Gaussian distribution N is given by

$$N(\mu_{jm},\, \Sigma_{jm},\, o_t) = \frac{e^{-0.5(o_t - \mu_{jm})\Sigma_{jm}^{-1}(o_t - \mu_{jm})}}{\sqrt{(2\pi)^n |\Sigma_{jm}|}}$$

$b_j(o_j)do_t$ is the probability of the j^{th} state generating the observation vector in the set $[o_t, o_t + do_t]$. The conditions that need to be satisfied are:

$$c_{jm} \geq 0,\ 1 \leq j \leq N,\ 1 \leq m \leq M\ \sum_{m=1}^{M} = 1,\ 1 \leq j \leq N$$

i.e, the weighting coefficients have to be positive and must sum up to one in each state.

- Initial state distribution, $\pi = \pi_i$, where,

  $$\pi_i = pq_1 = i,\ 1 \leq i \leq N$$

  i.e, the probability of the i_{th} state being the initial state. These conditions must be satisfied:

  $$\sum_{i=1}^{N} \pi_i = 1$$

  i.e, the initial distribution must sum up to one. Since the initial state is always the first state in case of left-to-right HMMs, therefore, the initial distribution π is given as [10...0]. The continuous density HMM which is given by λ is given as:

  $$\lambda = [A, c_{jm}, \mu_{jm}, \Sigma_{jm}, \pi] \tag{6.5}$$

Some of the problems with HMM are:

1. Evaluation Problem: It pertains to the calculation of probability of a set of O observations, where, $O = \{o_1, o_2, o_3, ..., o_T\}$ for a given Markov Model λ. Forward-Backward algorithm can be used to calculate the probability.
2. Decoding Problem: It pertains to finding the optimal state sequence of a HMM, λ for a given set of observations $O = \{o_1, o_2, o_3, ..., o_T\}$. "Single best state sequence" is the most used criteria for defining the optimality, where, $Q = \{q_1, q_2, q_T\}$ (this optimal state sequence can be found from Viterbi algorithm), which maximizes $P(Q|O, \lambda)$ or $P(Q,O|\lambda)$.
3. Training Problem: It pertains to finding out the optimal HMM parameters $\lambda = [A, c_{jm}, \mu_{jm}, \Sigma_{jm}, \pi]$, for a set of observations given as $O = \{o_1, o_2, o_3, ..., o_T\}$. These parameters can be found from Baum-Welch Algorithm.

6.1.1.4 Neural Network

In the case of linear mapping, the samples in the feature space are projected in the classification space with the weights of the data sets determined through known bearing condition. In case of data belonging to the same class, *the least squared criterion* is used to create cluster effects. More information on this can be found from [4]. This however, does not guarantee a clear demarcation of the classes in the classification space by linear boundaries. There could be an overlapping of the patterns which belong to different classes in the classification space. This leads to the necessity of non-linear mapping in the classification space.

A three layered artificial neural network can be used to accomplish non-linear mapping from the feature space to the classification space. This artificial neural network represents the non-linear relationship between the input and the output. The fact that we can develop a non-linear relationship between the input and the output in the absence of sufficient system information is one of the biggest advantages of using neural networks. Training is the most important aspect of this neural network structure where most of the intense computation takes place. Once the training has been done, the network starts working fast for the identification of any unknown input samples; identifying the relation between any input data even in the presence of spurious signals.

Artificial Neural Networks(ANN)

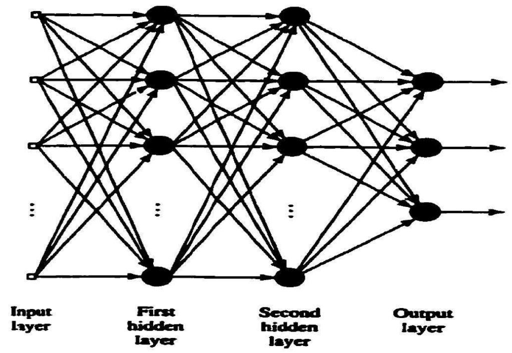

Figure 6.7 Multiplayer Neural Network Architecture with two hidden layers

ANN helps in describing a system when it becomes impossible to use analytical methods. They describe the system in terms of input and output. An ANN consists of several layers of neurons, an input layer, one or more hidden layers and an output layer. Details on this can be found in [4]. The output of first layer (input layer) is fed to the first hidden layer, whose output is fed to the next hidden layer and so on. Figure 6.7 [4] shows the architecture of multiplayer neural network with two hidden layers.

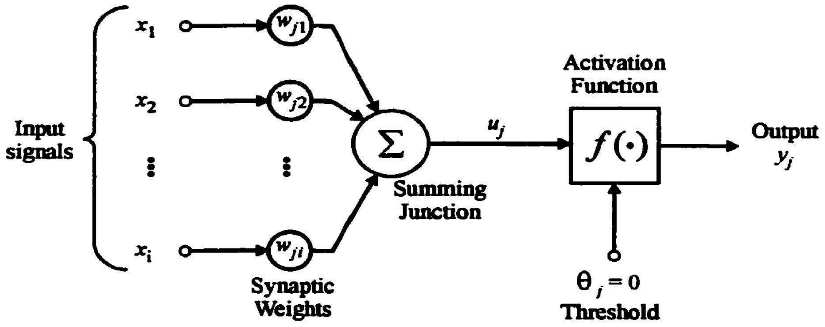

Figure 6.8 A Neuron Model

A fully connected network is one in which the neuron in one layer is connected to all the neurons or nodes in the previous layer. The signal flows in the forward direction from layer to layer. **Neuron** is an information processing unit for the operation of the neural network. Figure 6.8 [4] shows one such neuron model. The three elements to the neuron model are:

1. *Synapses* or *connecting links*, which is characterized by weight of its own. For example, a signal x_i at the input of synapse i connected to neuron j is multiplied by the synaptic weight w_{ji}, where j is the neuron in question and i refers to the input end of the synapse.
2. An *adder* for summing the input signals, weighted by the respective synapses of the neuron. This forms a linear combiner.

3. An *activation function* which limits the output of a neuron. Except for the input, every neuron has an activation value which is the weighted sum of the input signals [4]. The amplitude range of the output signal is limited to some finite value because of the activation function. Generally, the amplitude range of the output of a neuron is written as the closed interval $[0, 1]$ or $[-1, 1]$ [4] Mathematically, neuron j may be described as

$$u_j = \sum_{i=1}^{I} w_{ji} x_i \tag{6.6}$$

and

$$y_i = f(u_j - \theta_j) \tag{6.7}$$

where,

x_1, x_2, ..., x_1 are the input signals

w_{j1}, w_{j2}, ..., w_{jI} are the synaptic weights of the neuron

u_j is the linear combiner output

θ_j is the threshold

$f(.)$ is the activation function

yj is the output signal.

v_j, the internal activity level, is the linear combiner output u_j modified with the threshold θ_j:

$$v_j = u_j - \theta_j \tag{6.8}$$

Equations 6.6 and 6.7 can be combined to give

$$v_j = \sum_{i=1}^{I} w_{ji} x_i \tag{6.9}$$

and

$$y_i = f(v_j) \tag{6.10}$$

$f(.)$ is the activation function which denotes the output of a neuron in terms of the internal activity level at its input. The activation function could be *threshold function*, *Piecewise-Linear Function* and *Sigmoid Function.*

MultiLayer Feedforward Artificial Neural Network

They are used to solve complicated problems through supervised training with a popular algorithm called the *error back-propagation algorithm.* This algorithm helps in training multilayer perceptrons. Training of feed forward network takes place in an iterative fashion, where, each iteration cycle involves forward propagation path followed by an error backward-propagation pass to update the weights [4]. When the input nodes receive their activation function levels in the form of input patterns, the propagation starts, which proceeds through hidden layers up to the output levels by computing the activation levels of the nodes in each of those layers. The outputs are produced at the end of it which gives the actual response of the system. There is no change in the synaptic weight during this propagation. Weight adjustment is brought by the propagation of the error function of the output back through the net and modifying all the weights. The iterative method propagates error function required to adapt weights back from the nodes in the output layers to nodes in the hidden layers in accordance with the training rule [4]. In order for the actual response to move closer to the desired response the weights are adjusted. The adjustments of the training sets are done until the error criterion is met. Once the training is done, it is possible to relate any input pattern with an appropriate output pattern. The trained network would give an output when an input sample is presented to it. A new input would lead to an output with features that are similar to input vectors with similiar features used in training. Therefore, the training can be done on a certain set of input/output pairs without including all the input/output pairs.

Back-Propagation Training Algorithm

The NN has to compute the error derivative of the weights in order to train a NN, so that the error between the desired and actual output is reduced. The derivative pertains to calculating the error changes as each weight is increased or decreased. The back propagation algorithm is the most widely used method for computing this error derivative. It is easiest to understand the back-propagation algorithm if the network is linear. Each of the error derivatives of the weights is computed by calculating the error activity, which is the difference between the actual and desired output. In order to compute the error activity of a hidden unit in the just before the output layer, all the weights between that hidden unit and the output units to which it is connected is identified. These weights are then multiplied by the error activity function of those output units and add the products. This would give the error activity of the particular hidden unit. We can similarly compute in like fashion the error activity for other layers, moving from layer to layer in a direction opposite to the way activities propagate through the network after calculating all the error activities in the hidden layer just before the output layer, hence, giving it the name of “back-propagation”. The error derivative of the weight for each of the incoming connection is calculated once the error activity is calculated. The Error derivative is the product of the error activity and the activity through the incoming connection. Gradient descent method is used for implementation of back-propagation algorithm. The effectiveness and convergence of this algorithm depends on the value of learning rate constant η. Though gradient descent is an efficient method for obtaining the weight values that minimizes error, but there in no constant value of η suitable for all the cases causing errors which reduce the convergence rate.

Radial Basis Function Neural Network (RBFNN)

In case of RBFNN, the activation of the hidden unit is determined by the distance between the input vector and the prototype vector. It is basically a nearest neighbor classifier. The structure of a Radial Basis Function is as follows:

$$f(y, \alpha) = exp(-\frac{\sum_k |y_k - \mu|^\alpha}{N\theta_\alpha}) \tag{6.11}$$

where the exponent parameter $\alpha \: \epsilon \: (0, \infty)$; and μ and θ_α are the center and α_{th} central moment of the data set, respectively. f() becomes Gaussian, for $\alpha = 2$ which is the typical radial basis function used in the neural network. For any application, the first task is to calculate the mean and the central moment from the sampled time series data when the dynamical system is in the nominal condition. The mean μ and the central moment θ_α are calculated as:

$$\mu = \frac{1}{N} \sum_{k=1}^{N} y_k \tag{6.12}$$

and

$$\theta_\alpha = \frac{1}{N} \sum_{k=1}^{N} |y_k - \mu|^\alpha \tag{6.13}$$

The distance between any vector y and the center i is obtained as

$$d\,(y, \mu) \equiv (|y(n) - \mu|^\alpha)^{\frac{1}{\alpha}} \tag{6.14}$$

From equation 6.11, the RBF at the nominal condition is: $f_0 = f(y)$. Under all conditions, the mean and central moment is constant.

Online Adaptive Reformulation is one of the biggest advantages of using Neural Networks compared to statistical based methods. This gives it the *flexibility* which cannot be achieved through statistical methods. It also eliminates the need for batch processing. But designing an effective neural network system has always been a challenging task. Back-propagation and RBF give a classification rate of 71.8% and 73.2% respectively [27]. In the case of back-propagation NN, the entire set of data is used for classification, which eventually becomes a time consuming process if the data is large, where as, in the case of RBF, the accuracy achieved is less on account of the dimensioanlity reduction in the data.

Competitive Neural Network

In *competitive learning*, the output neurons of a NN compete among themselves to be fired. Details on this can be got from [26]. In case on a NN based on *Hebbian Rule*, several of the output neurons may be active at the same time, where as in competitive learning only a single output neuron is active at any instant of time. This makes it very useful to discover statistically salient features that can be used to classify a set of input patterns. The basic elements of a competitive learning rule are:

- A set of neurons that are same except for the randomly distributed synaptic weights, and hence give different response to a given set of input patterns.
- A *limit* imposed on the "strength" of each neuron.
- A mechanism that permits neurons to compete for the right to respond to a given input, such that only one neuron is active at any given time.

In its simplest form, competitive learning NN has a single layer of output neurons, each of which is fully connected to the input nodes. For a neuron k to be the winning neuron, its induced local field v_k for a specified input pattern x must be the largest among all the neurons in the network. The output signal y_k of winning neuron k is set to one; the output signals of all the neurons that lose the competition are set to 0.

$$y_k = 1 \text{ for all } j,\, j \neq k$$

$$y_k = 0 \text{ otherwise}$$

where the induced local field v_k represents the combined action of all forward and feedback inputs to neuron k

Let w_{kj} denote the synaptic weight connecting the input node j to neuron k. If all synaptic weights are positive, then

$$\sum_j w_{kj} = 1 \text{ for all k}$$

A neuron learns by shifting synaptic weights from its inactive to active input nodes. Learning does not take place if a neuron does not respond to a particular input node. If a particular neuron wins the competition, each input node of that neuron relinquishes some proportion of its synaptic weight, and the weight relinquished is then distributed equally among the active input nodes [26]. According to the competitive learning rule, the change (Δw_{kj}) in weight applied to the synaptic weight (w_{kj}) is given as

$$\Delta w_{kj} = \eta \left(x_j - w_{kj}\right) \text{ if neuron } k \text{ wins the competition}$$

$$\Delta w_{kj} = 0 \text{ if neuron } k \text{ loses the competition}$$

where, η is the learning-rate parameter. This causes the synaptic weight vector w_k of the winning neuron k to move in the direction of the input pattern x. This neural network also brings about *clustering.* However, for clustering to happen in a stable manner, the input patterns must fall into distinct groupings to begin with; otherwise the network will be unstable. Neural Network has been used in this thesis because it can handle data which may be distorted and noisy and at the same time can be used for operation in real time mode.

CHAPTER 7

EXPERIMENTAL RESULTS

Once the analysis of the data is done using a two stage neural network, it is necessary to evaluate the performance of the fault classifier. This is done through the performance metrics - Confusion Matrix, Receiver Operating Characteristics and finally Health Index.

7.1 Implementation

The implementation involves recording the voltage values in the case of electrical test bed and recording the vibration values for the motor in the case of mechanical test bed over a period of five days. For recording these values, the test beds as explained in chapter 2 were used.

7.2 Performance Analysis

7.2.1 Classification of the Input vectors

A classifier maps a list of measured features into a classification state. Figure 7.1 shows the classification of the input data after passing through the artificial neural network, where the x, y and z axes represent the x, y and z component of the vibration data respectively. And figure 7.2 shows the classified data for the electrical test bed, where x and y represent the x and y values of the two dimensional voltage data. Artificial Neural Network Classifiers implement non-linear decision boundaries which use "K-nearest neighbor" discriminant function analysis to benchmark the neural network's performance. The nearest neighbor classifier can be explained as follows: If it is required to classify an unknown vector x, where a number of classes are represented by example points in a feature space vector, then this is done by finding the point closest to x and assigning the closest point's class to it. In K-nearest neighbor, nearest K points to x are found, and x gets assigned the class which is represented by the largest number of neighboring points. This classification of data paves the way for formulation of confusion matrix (with the help of testing data) and finally the Receiver Operating Characteristics. Confusion matrix is used to evaluate the algorithm proposed in the thesis. Health Index is another method for evaluating the performance of the machine.

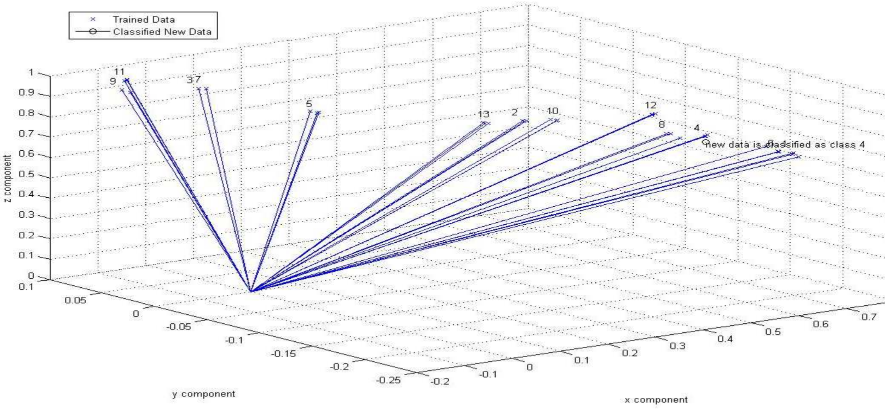

Figure 7.1 Classified Output-Mechanical Test Bed

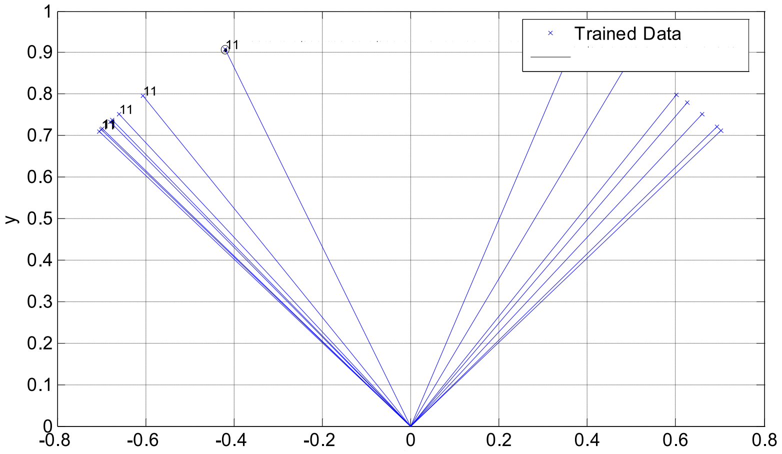

Figure 7.2 Classified Output-Electrical Test Bed

7.2.2 Confusion Matrix

Confusion matrix is a visualization tool used for performance evaluation. Details on this can be obtained from [27] [50] [51] [52]. It gives a degree of correlation between various parameters such as features, classes, etc. It is a square matrix where the entries represent the degree of correlation between its *ith* and *jth* element. The number of rows and columns is equivalent to the number of classes. The columns represent the system's classification where as the rows represent the true classification. For a perfect system, only the diagonal elements will be present in the confusion matrix, where as, the presence of off diagonal elements indicates misclassification. The sum of all the elements is equal to the number of testing data. The entries (c_{ij}) give the data which are actually of class i but are classified as class j by the Neural Network System. Thus, it allows the user to understand the manner in which the classes have been confused with each other. The entries of the confusion matrix as shown in figure 7.3 is explained as follows:

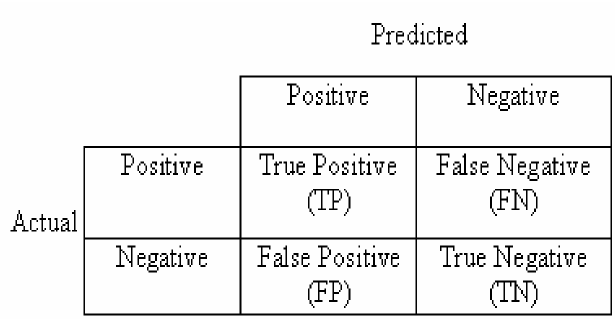

		Predicted	
		Positive	Negative
Actual	Positive	True Positive (TP)	False Negative (FN)
	Negative	False Positive (FP)	True Negative (TN)

Figure 7.3 Confusion Matrix

True Positive (TP) gives the number of correct predictions; False Positive (FP) gives the number of incorrect predictions; False Negative (FN) gives the number of misses and True Negative (TN) is the number of correct rejections. Out of all the recorded data, some data sets were chosen for testing the performance of the two stage neural network. This method of formulating the Confusion Matrix is called the *Generalization Test.* After training, the testing data set of known categories is passed through artificial neural network classification system in order to find the number of correct and incorrect classifications for each class for getting the TP and FP rates. Figure 7.4 shows the confusion matrix for the testing data from which the true positive rate (hits) and false positive rate (wrong predictions) can be determined to get the *Receiver Operating Characteristics* (ROC) as shown in figures 7.5 and 7.6.

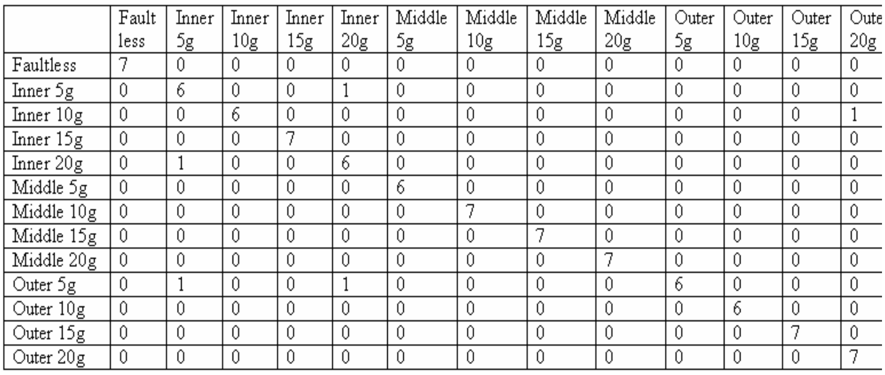

	Fault	Inner	Inner	Inner	Inner	Middle	Middle	Middle	Middle	Outer	Outer	Outer	Oute
	less	5g	10g	15g	20g	5g	10g	15g	20g	5g	10g	15g	20g
Faultless	7	0	0	0	0	0	0	0	0	0	0	0	0
Inner 5g	0	6	0	0	1	0	0	0	0	0	0	0	0
Inner 10g	0	0	6	0	0	0	0	0	0	0	0	0	1
Inner 15g	0	0	0	7	0	0	0	0	0	0	0	0	0
Inner 20g	0	1	0	0	6	0	0	0	0	0	0	0	0
Middle 5g	0	0	0	0	0	6	0	0	0	0	0	0	0
Middle 10g	0	0	0	0	0	0	7	0	0	0	0	0	0
Middle 15g	0	0	0	0	0	0	0	7	0	0	0	0	0
Middle 20g	0	0	0	0	0	0	0	0	7	0	0	0	0
Outer 5g	0	1	0	0	1	0	0	0	0	6	0	0	0
Outer 10g	0	0	0	0	0	0	0	0	0	0	6	0	0
Outer 15g	0	0	0	0	0	0	0	0	0	0	0	7	0
Outer 20g	0	0	0	0	0	0	0	0	0	0	0	0	7

Figure 7.4 Confusion Matrix of testing data for the Mechanical Test Bed

ROC is a plot of the classifier's TP rate (sensitivity) against the FP rate (specificity). Sensitivity is defined as $\frac{TP}{TP+FN}$ and Specificity is defined as $\frac{FP}{FP+TN}$. High sensitivity means that the classifier identifies most of the positive samples and its performance is good, where as high specificity means that the classifier identifies most of the negative samples and its performance is poor. The curve always goes through two points $(0, 0)$ and $(1, 1)$. $(0, 0)$ is the point at which no positives are found by the classifier, where as $(1, 1)$ gives the point where the classifier finds everything as positive. At $(0, 0)$, the classifier identifies all the negative cases correctly but the positive cases are identified incorrectly, where as

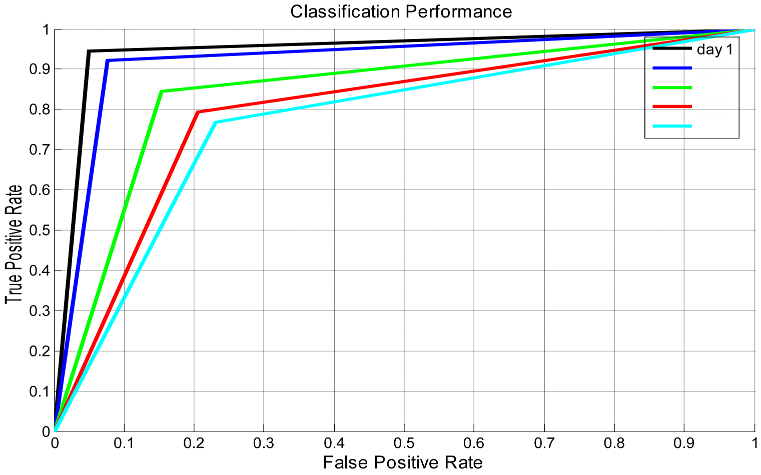

Figure 7.5 Receiver Operating Characteristics of the Mechanical Test Bed

at (1, 1), the classifier identifies all the positive cases correctly but the negative cases get identified incorrectly. The graph on figure 7.5 shows the ROC for the mechanical test bed for each of the five days during which the experiment was performed. Figure 7.6 shows the same for the electrical test bed. It can be clearly inferred from the graphs that the condition of the motor deteriorates as the days proceed, i.e, the ROC curve is higher for day 1 compared to day 5. As already explained, the best performance is achieved near the point (0, 1). The multi-class task learning vector quantization is reduced to the binary decision, i.e., either it belongs to a desired class or it does not, irrespective of the number of classes present.

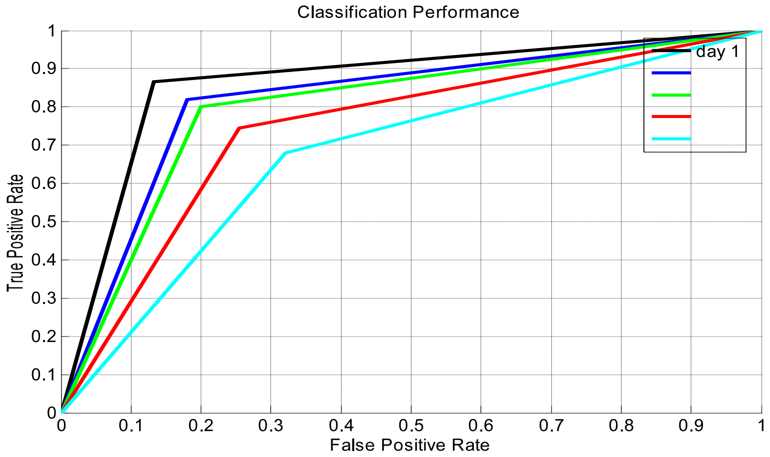

Figure 7.6 Receiver Operating Characteristics of the Electrical Test Bed

7.2.3 Health Index

Health index is also plotted to evaluate the performance of the machine. In the case of mechanical test bed it is computed by adding weights to various regions of the metallic disc simulating the faulty bearing, and in the case of electrical test bed it is done by varying the value of inductance during the course of experiment. The health index as the name indicates tells the state of the machine under a particular loading condition. Further information can be obtained from [53]. It checks the condition of the motor under no load and then uses a fault dictionary to facilitate the use of pattern recognition techniques to diagnose the faults. Signal behavior characteristics can be used to study the condition of the motor under no-load (faultless) and loaded (fault) condition by which we can get the heath index to get the deviation from the normal condition. The health index is calculated using:

$$HV(faultless) = \sqrt{[(\sum_i(((faultless_i - Y_n)/Y_n)_j \times 0.1)^2)/(N-1)]} \tag{7.1}$$

where,

$$j = 1, 2, 3, ...N$$

$$Y_n = mean$$

$$faultless_i = \text{ith sampled response}$$

Thus, $HV(faultless)$ is the faultless value which acts as the reference for the system.

For the loaded system (system under fault), the equation would be given by,

$$HV(fault) = \sqrt{[(\sum_i(((fault_i - Y_n)/Y_n)_j \times 0.1)^2)/(N-1)]} \tag{7.2}$$

The health index if the system can therefore be calculated as

$$HI = \tfrac{HV(faultless)}{HV(fault)} \text{ if } HV(faultless) < HV(fault)$$

$$HI = 1 \text{ if } HV(faultless) > HV(fault)$$

Figures 7.7 and 7.8 show the health index plot for the mechanical and electrical test bed respectively. It is clear from this figure that the health index would range between Zero (poor) and 1 (fine), giving an indication of the health of the system. For the experiments performed in the lab it was found that the health index was larger for smaller values of weights applied on the inner ring compared to the larger value of weights which were applied on the outer ring, in the case of mechanical test-bed; and it was larger for smaller value of inductances as compared to the larger values of inductances in the case of electrical test-bed. This also implies that the vibrations produced are lesser when the weights are applied on the inner

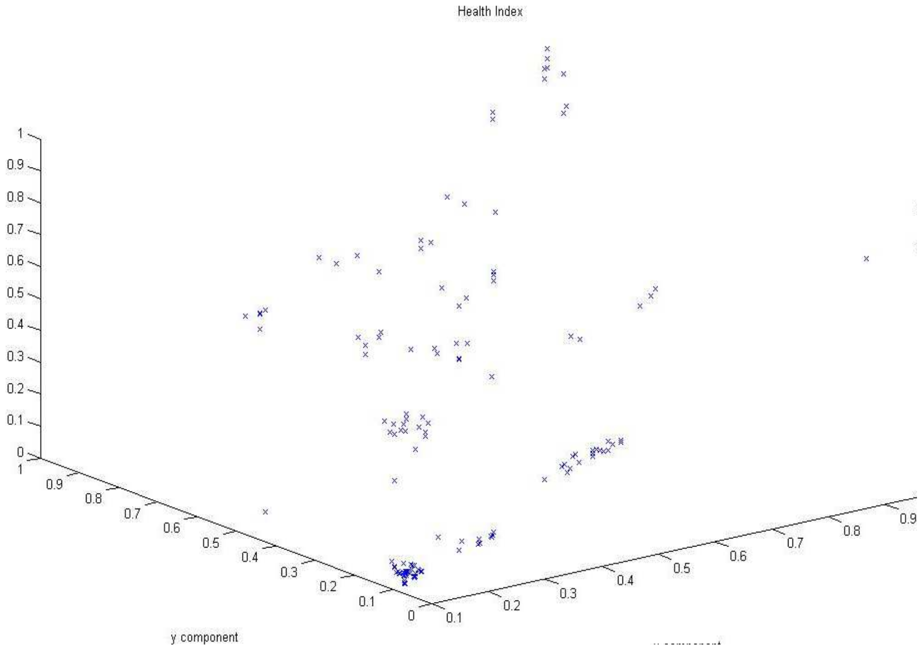

Figure 7.7 Health Index for the Mechanical Test Bed

ring as opposed to those applied on the middle and outer rings respectively in the case of mechanical test bed experimentation. Similarly, the value of fault voltage obtained is greater when the value of the external inductance added is higher in value as in the case of electrical test bed. This would help condition monitoring systems to be implemented, where maintenance action can be brought into service at some predetermined value of failure. During failure, the latest response can be assigned as the cause for diagnosis. The trend obtained from this polt can be used for fault prognosis.

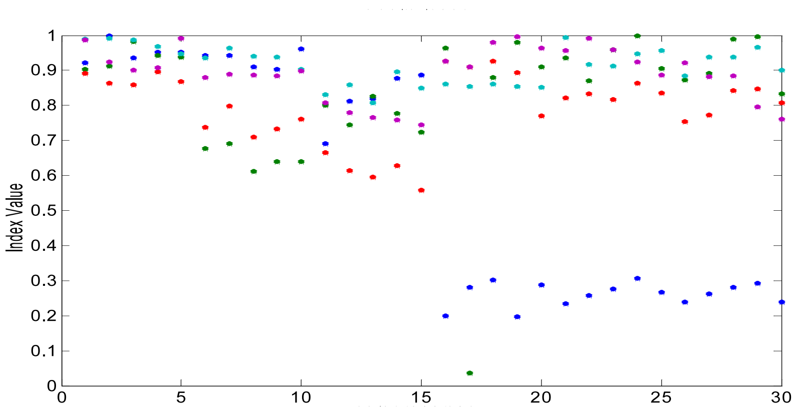

Figure 7.8 Health Index for the Electrical Test Bed

CHAPTER 8

CONCLUSION AND FUTURE WORK

This research work proposes diagnosis and prognosis of bearing faults and stator winding faults using Wireless Modules and Wireless Sensors, where in, a novel two stage neural network has been used to analyze the vibration data and the voltage values obtained from the mechanical and electrical test-bed setup respectively. The work suggests an experimental setup which is a low cost approach for emulating bearing fault and short circuit current fault in a motor; to wirelessly sense the vibrations and voltages produced due to these faults. The fault classification algorithm used has certain features such as: (a) Using PCA rather than conventional statistical methods to reduce the dimensionality of the data, (b) A method which estimates and recursively calculates the principal components, hence, giving robustness in the diagnosis, (c) Use of Supervised Learning Quantization which has a fast processing time, (d) Finally, Receiver Operating Characteristics is plotted and the health index is computed to find the condition of the motor at a given instant. One of the features that could be used in the future is the use of energy efficient wireless sensors and modules in order to make the Condition Based Maintenance more effective. The sampling rate of the wireless modules for vibration and voltage measurement could be increased further by using a SD card which would store the values and then transmit to the computer; The vibration measurement is basically the measurement of sound, so there could be better reproduction of the signals obtained from the machine if a wireless module is programmed with a sampling rate of more than $7K$ (Nyquist Criterion).

Since, in the measurement of vibration, the value of g(center of gravity) plays a very significant role, comparative studies can be done if the entire experiment is done in a new environment as this would give a set of values with different center of gravity-giving the extent to which the center of gravity has an effect on the readings, this could also show the effect of external parameters on the readings obtained. In this thesis we have considered only two type of faults in the induction motor- one each for electrical and mechanical. We could also consider other fault types to determine the classifier performance for indicating the condition of the motor at any instant of time. Last, the experiment has been conducted on induction motor since its widely used in the industry and has simple and rugged construction, we could examine the classifier performance by performing the experiments on other types of motor like the synchronous motor.

REFERENCES

[1] A. Tiwari, P. Ballal, and F. L. Lewis, “Energy-efficient wireless sensor network design and implementation for condition-based maintenance,” vol. 1, 2007, pp. 1–23.

[2] P. Ballal and F. Lewis, *Wireless Sensor Network Design.* Pearson Education, to be published.

[3] http://www.bmpcoe.org/bestpractices/internal/arlps/arlps7.html.

[4] C. Ping, “Bearing condition monitoring and fault diagnosis,” Master’s thesis, University of Calgary (Canada), 2001.

[5] R. Samsi, “A probabilistic framework for fault detection in induction motors,” Ph.D. dissertation, The Pennsylvania State University, 2006.

[6] O. Hasan, “Fault detection, diagnosis and prognosis of rolling element bearings: Frequency domain methods and hidden markov modeling,” Ph.D. dissertation, Case Western Reserve University, 2004.

[7] P. D. McFadden and J. D. Smith, “Model for the vibration produced by a single point defect in a rolling element bearing,” *Journal of Sound and Vibration*, pp. 69–82, 1984.

[8] H. R. Martin and F. Honarvar, “Application of statistical moments to bearing failure detection,” vol. 44, 1995, pp. 67–77.

[9] R. B. W. Heng and M. J. M. Nor, “Statistical analysis of sound and vibration signals for monitoring rolling element bearing condition,” vol. 53, 1998, pp. 211–226.

[10] P. D. McFadden and J. D. Smith, "Vibration monitoring of rolling element bearings by high frequency resonance technique-a review," vol. 77, 1984, pp. 3–10.

[11] I. Howard, "A review of rolling element bearing vibration: Detection, diagnosis and prognosis," 1994.

[12] E. A. Seyfettin, "Multisensor fusion for induction motor aging analysis and fault diagnosis," Ph.D. dissertation, The University of Tennessee, 1999.

[13] C. J. Li and J. Ma, "Wavelet decomposition of vibrations for detection of bearing localized faults," vol. 30, 1997, pp. 143–149.

[14] ——, "Bearing localization defect detection by bicoherence analysis of vibrations," *Journal of Engineering for Industry*, vol. 117, pp. 625–629, 1995.

[15] G. Godi, B. Li, M. Y. Chow, and J. C. Hung, "Motor bearing diagnosis by a fundamental frequency amplitude based fuzzy decision system," vol. 4, 1998, pp. 1961–1965.

[16] *Vibration analysis via neural network inverse models to determine aircraft engine unbalance condition*, vol. 4, 2003.

[17] I. E. Alguindigue, A. Loskiewicz-Buczak, R. E. Uhrig, L. Hamon, and F. Lefevre, "Vibration monitoring of edf rotating machinery using artificial neural networks," 1991.

[18] D. H. Hanson, "Artificial neural network based survival analysis for hydromechanical systems," Ph.D. dissertation, The University of Iowa, 2004.

[19] M. Subrahmanyam and C. Sujatha, "Using neural networks for the diagnosis of localized defects in ball bearings," vol. 30, 1997, pp. 739–752.

[20] http://images.google.com/imgres?imgurl=http://mvpprograms.com/help/images/KurtosisPic

[21] L. I. Smith, *A tutorial on Principal Component Analysis.*

[22] M. H. Fredric and K. Ivica, *Principles of Neurocomputing for Science and Engineering.* McGraw-Hill.

[23] M. A. Turk and A. P. Pentland, “Face recognition using eigenfaces,” pp. 586–591.

[24] ——, “Eigenfaces for recognition,” vol. 3(1), 1991.

[25] T. Sanger, “Optimal unsupervised learning in a single layer linear feedforward neural network,” vol. 12, 1989, pp. 459–473.

[26] S. Haykin, *Neural Networks A Comprehensive Foundation.* Pearson Education, 2003.

[27] P. S. Dang, “A potential field approach for distributed control of discrete actuator and sensor arrays,” Ph.D. dissertation, University of Texas at Arlington, 2007.

[28] S. Chitroub, A. Houacine, and B. Sansal, “Principal component analysis of multispectral images using neural networks,” pp. 89 – 95.

[29] E. Oja, “Neural networks principal components and subspaces,” *Intenational Journal of Neural Systems*, pp. 61–68, 1989.

[30] ——, “A simplified neuron model as a principal components analyzer,” *Journal of Mathematical Biology*, pp. 267–273, 1989.

[31] http://www.cs.helsinki.fi/u/ahyvarin/whatisica.shtml.

[32] V. J. Stone, *Independent Component Analysis: A Tutorial Introduction.*

[33] J. Shlens, *A tutorial on Principal Component Analysis.*

[34] M. T. Hagan, H. B. Demuth, and M. Beale, *Neural Network Design.* PWS Publishing Company.

[35] http://www.statsoft.com/textbook/glosc.htmlClassification.

[36] http://www.gc.ssr.upm.es/inves/neural/ann1/concepts/Suunsupm.htm.

[37] http://pagesperso-orange.fr/polyvalens/clemens/wavelets/wavelets.html.

[38] http://www.astro.princeton.edu/esirko/idlhtmlhelp/examples3.html.

[39] F. A. K. A. Badour, "Application of wavelet techniques to vibration analysis of rotating machines," Master's thesis, King Fahd University of Petroleum and Minerals, December 2007.

[40] S. Bhunia, K. Roy, and J. Segura, "A novel wavelet transform based transient current analysis for fault detection and localization," New Orleans Louisiana USA, 2002, pp. 0–412.

[41] I. Daubechies, *Ten Lectures on Wavelets*, ser. CBMS-NSF Reg. Conf. Ser. Appl. Math. 61. Philadelphia, PA: SIAM, 1992.

[42] R. Rao and A. Bopardikar, *Wavelet Transforms: Introduction to Theory and Applications Reading.* Massachussets, MA: Addison-Wesley, 1998.

[43] M. E. H. Benbouzid and H. Nejjari, "A simple fuzzy logic approach for induction motors stator condition monitoring," 2001, pp. 634 – 639.

[44] D. Sauter, N. Mary, F. Sirou, and Thieltgen, "Fault diagnosis in systems using fuzzy logic," vol. 2, 1994, pp. 883 – 888.

[45] *A fuzzy diagnostic System: application to linear induction motor drives*, vol. 1, 1997.

[46] G. G. et al., "Motor bearing fault diagnosis by a fundamental frequency amplitude based fuzzy decision system," vol. 4, 1998, pp. 1961–1965.

[47] M. Zeraoulia, A. Mamoune, H. Mangel, and M. E. H. Benbouzid, "A simple fuzzy logic approach for induction motors stator condition monitoring," *Journal of Electrical Systems*, pp. 15–25, 2005.

[48] J. M. Mendel, "Fuzzy logic systems for engineering: a tutorial," vol. 83, 1995, pp. 345–377.

[49] A. W. Drake, *Fundamentals of Applied Probability Theory.* NewYork: McGraw-Hill Company, 1967.

[50] A. Zaknich, *Neural networks for intelligent signal processing: World Scientific Singapore.* John Wiley and Sons Inc., 2003.

[51] G. Vachtsevanos, F. Lewis, M. Roemer, A. Hess, and B. Wu, *Intelligent Fault Diagnosis and Prognosis for Engineering Systems.* John Wiley and Sons Inc., 2006.

[52] C. Chen, *Signal and image processing for remote sensing.* CRC Press Technology and Industrial Arts, 2006.

[53] A. Davies, *Handbook of Condition Monitoring: Techniques and Methodology.* Chapman and Hall, 1998.

BIOGRAPHICAL STATEMENT

Akarsha Ramani received her Bachelor of Engineering degree in Electrical and Electronics Engineering from Anna University, 2005. She pursued her Master of Science in University of Texas at Arlington, where she worked as a Graduate Research Assistant at Automation and Robotics Research Institute.